INVESTIGATIONS OF THE HOST PROPERTIES OF THREE FLUORESCENT CAGE COMPOUNDS

A Thesis

Submitted to the Graduate Faculty

in Partial Fulfilment of the Requirements

for the Degree of

Master of Science

in the Department of Chemistry

Faculty of Science

University of Prince Edward Island

Charlottetown, PE

March 2007

Your file Votre référence
ISBN: 978-0-494-32106-5
Our file Notre référence
ISBN: 978-0-494-32106-5

The author has agreed that the Library, University of Prince Edward Island, may make this thesis freely available for inspection. Moreover, the author has agreed that permission for extensive copying of this thesis for scholarly purposes may be granted by the professor of professors who supervised the thesis work recorded herein or, in their absence, by the Chair of the Department or the Dean of the Faculty in which the thesis work was done. It is understood that due recognition will be given to the author of this thesis and to the University of Prince Edward Island in any use of the material in this thesis. Copying or publication or any other use of the thesis for financial gain without approval by the University of Prince Edward Island and the author's written permission is prohibited.

Requests for permission to copy or to make any other use of material in this thesis in whole or in part should be addressed to:

Chair of the Department of Chemistry

Faculty of Science

University of Prince Edward Island

Charlottetown, PE

Canada C1A 4P3

SIGNATURE PAGE

(ii)

REMOVED

SIGNATURE PAGE

(iii)

REMOVED

Abstract

Supramolecular chemistry has been an emerging field over the last twenty years with host-guest inclusion being the simplest example. Usually in fluorescence-based host-guest inclusion studies the host is a non-fluorescent cage compound and the effects of inclusion on fluorescent guests are investigated. However, in this project three fluorescent cage compounds were identified for study. This enabled the investigation of their host properties using non-fluorescent guests, to determine the effect of their inclusion on the host fluorescence. The ability of such fluorescent hosts to form complexes has potential application in fluorescent nanomachines and molecular switches and sensors.

The first host investigated was the methoxy nanoball, which displayed both a ligand centered and a ligand-to-metal charge transfer band and which was found to form a weak 1:1 complex with benzene. This band also displayed significant pH dependence, indicating a potential application as a molecular controlled pH sensor. Benzene was the only guest investigated which formed a complex with the nanoball, and because it was a weak complex it was concluded that methoxy nanoball was not a good host for inclusion. However, guest encapsulation during the nanoball synthesis was attempted and proved to be promising, especially with pyrene.

The compound LB[6] also possessed fluorescence properties and formed a higher order complex with the fluorescent guest curcumin. LB[6] also gave interesting but scattered thermodynamic results with the binding constant (K) value both increasing and decreasing with temperature. Time-resolved fluorescence results confirmed previous steady-state

results with a small increase in intensity with increasing benzene concentration.

The bistren cage compound displayed fluorescence which was sensitive to the polarity of the guests with which it formed higher order complexes. This host also gave good thermodynamic data with anisole, where the K value decreased with increasing temperature. Also, the time-resolved fluorescence showed a trend of decreasing lifetime (ns) with increasing concentration of aniline.

Acknowledgements

First I would like to sincerely thank Dr. Brian Wagner for taking me under his wing three years ago and being a mentor to me ever since. He allowed me to work independently and really made me feel that my work is truly important and that he has complete faith in my laboratory abilities. If I had not come in contact with such a caring, supportive supervisor I may not be in the position I am today with my research experience.

Secondly I would like to thank my supervisory committee: Dr. Nola Etkin for all her help with synthetic and NMR techniques and Dr. Robert Haines for his help in preparation of this thesis. I would also like to thank Dr. Russ Kerr and his group for their help with HPLC and NMR characterization. Also thanks goes out to Dawna Lund for all her technical support, NMR training and expertise with all the instruments in the lab. I would also like to thank NSERC for funding this research through a Canada Graduate Scholarship.

My family and friends have supported me through thick and thin and kept me going when times were tough - thank you. Last but certainly not least I would like to thank my lab mates for all their help and humour which helped the hours pass with ease.

Table of Contents

List of Figures

List of Tables

List of Abbreviations

CB[6]	cucurbit[6]uril
MNB	methoxy nanoball
5-(MIA)	5-methoxy isophthalic acid
LB[6]	cucurbit[6]uril analogue (lagonabit[6]uril)
9,10-BCA	9,10-bis(chloromethyl)anthracene
K	association constant
H	host
G	guest
ANS	anilino naphthalene sulphonate
TNS	toluidino naphthalene sulphonate
CD	cyclodextrin
NMR	nuclear magnetic resonance
HPLC	high pressure liquid chromatography
LMCT	ligand to metal charge transfer
MLCT	metal to ligand charge transfer
HOMO	highest occupied molecular orbital
LUMO	lowest unoccupied molecular orbital
LC	ligand centered
CT	charge transfer
$CDCl_3$	deuterated chloroform
HCl	hydrochloric acid
D_2O	deuterium oxide

I. *INTRODUCTION*

The main goal of this project is the investigation of the physical and spectroscopic properties of three specific host molecules. These three host molecules are of particular interest because they exhibit significant fluorescent properties. This situation involving a fluorescent host is not typical for fluorescence-based host-guest inclusion studies, which usually involve a fluorescent guest and a non-fluorescent host. The most commonly used host molecules, including cyclodextrins, calixarenes, and cucurbiturils, are all non-fluorescent. However three examples of fluorescent host molecules with which to work were found , either through literature review or collaborations. This has allowed for the opportunity to undertake these rare studies from the point of view of host fluorescence, and thus the ability to study a new, wider range of guest molecules, which do not need to fluoresce. Not only can their host-guest inclusion complexes be studied, but this may also lead to the design of fluorescent sensors for the detection of non-fluorescent target compounds. It is also possible to study guest fluorescence in the range where these hosts do not fluoresce; this allows for a double experimental approach in such cases.

Host-guest inclusion can be defined as the phenomenon in which a small guest molecule becomes incorporated inside the cavity of a larger, cage-like host molecule. The binding between the host and guest is relatively weak, consisting in general of intermolecular forces, including van der Waals forces and hydrogen bonding.[1] Thus, there is an equilibrium established between the complex and the free host and guest molecules. The specific systems of interest in this project are those involving three specific host

molecules, namely methoxy nanoballs, a cucurbit[6]uril analogue and a bistren cage with a wide variety of non-fluorescent probes as guest molecules. These three hosts will be briefly introduced here, then described in more detail in section I.5.

Nanoballs were first synthesized by Zaworotko and co-workers in 2001.[2,3] These spherical structures are essentially finite spherical polyhedra. The nanoballs themselves are made by modular self-assembly of copper metal nodes and various isophthalic acid ligands. The methoxy nanoball is composed of copper metal nodes and 5-methoxy isophthalic acid ligands as seen in Figure 1. The result is a hollow ball with pits on the surface, which resembles a "molecular wiffle ball". These nanoballs have a huge potential to be used as hosts in host-guest inclusion chemistry due to the large number of pits available as potential interaction sites for guests. The nanoballs are substituted, discrete entities themselves but can also be joined to other nanoballs by spacer ligands to form complex 3D coordination polymers. Any such complex polymers formed would have an even greater number of cavities available as potential interaction sites for host-guest complexes to be formed.

a) b)

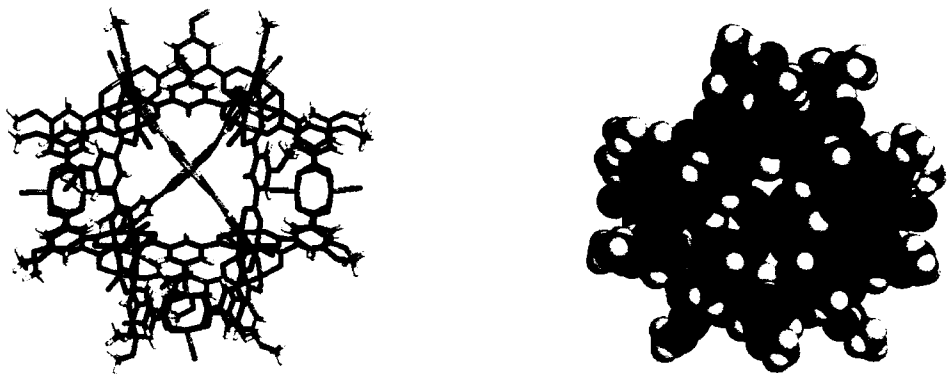

Figure 1 a) Crystal structure and b) space filling model of the methoxy nanoball

The structure of the cucurbit[6]uril (CB[6]) analogue seen in Figure 2 shows the elongated shape of the CB[6] analogues, with dimensions of 5.90x11.15x6.92 Å, compared to the cylindrically shaped CB[6]. This CB[6] analogue is expected to combine the advantageous features - tight binding, high selectivity, and unusual dynamics - of two important classes of host molecules, namely, cucurbiturils and cyclophanes.[4-6] Since these CB[6] analogues (like nanoballs) are intrinsically fluorescent, these compounds have been used by this research group in collaboration with the Isaacs research group as host molecules to study the binding properties of a wide variety of guest molecules.

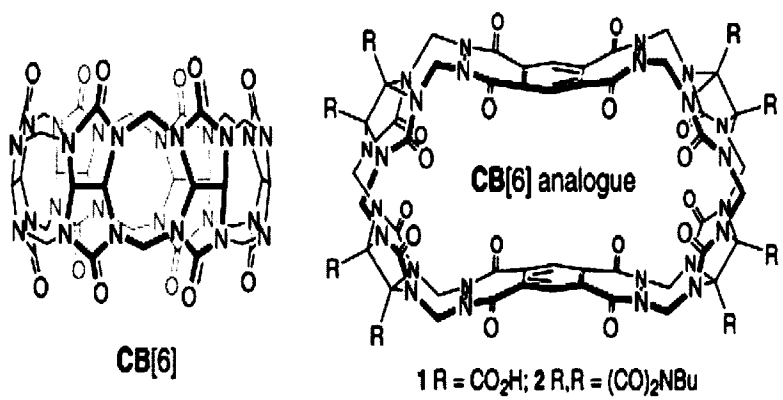

Figure 2 CB[6] analogue structure (on right)

(Reproduced from reference 45)

Another excellent example of an intrinsically fluorescent host is the bistren cage compound, seen in Figure 3, first prepared by Fabbrizzi *et al.*[7] This interesting compound contains the highly fluorescent fluorophore 9,10-substituted anthracene as part of its cage architecture. This cage compound has excellent host capabilities. Furthermore, it is highly fluorescent, although only under specific conditions. Bistrens are an important class of polyamine cages in which two tripodal tetramine subunits of the tren type (tren: 2,2',2"-triaminotriethylamine) are linked through their peripheral amine groups by three spacers R. The nature of R (an aliphatic chain) determines the dimensions of the ellipsoidal cavity and controls the rigidity of the system. Although Fabbrizzi considered metal binding, no inclusion complexes of this host with organic guests have been reported.

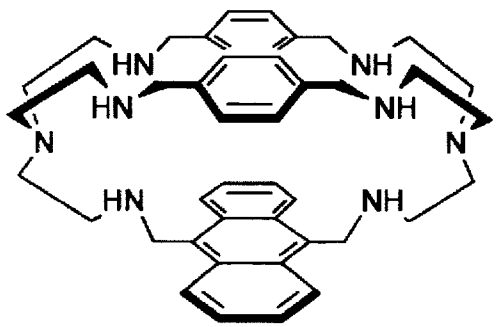

Figure 3 Bistren cage complex

(Reproduced from reference 7)

In this project, fluorescence spectroscopy is used to study the supramolecular host properties of the above mentioned types of host molecules. The purpose of this project is to characterise the properties of fluorescent hosts and examine their interactions with a range of non-fluorescent guest molecules. The ultimate goal in each case would be to join these hosts together using guests with multiple binding sites (eg. biphenyl). These systems would be analogous to coordination polymers where the hosts would be comparable to the metal nodes and the biphenyl (or other guests with two binding sites) would be comparable to the bidentate ligands. Potentially these host-guest complexes can be used to design fluorescent nanostructures or nanomachines by inclusion of guests to form 2:1 (or higher order) host-guest complexes.

I.1 *Supramolecular Chemistry*

Most chemistry is concerned with the structures and properties of molecules and the formation of covalent bonds to make new molecules. Recently research has been done on exactly how individual molecules can join together, *via* non-covalent interactions, to form larger more complex structures. This new scientific discipline is called supramolecular chemistry, and can be defined as "chemistry beyond the molecule".[1] This field of chemistry is concerned with the formation of new supramolecular structures using non-covalent intermolecular forces, including electrostatic interactions, van der Waals forces, hydrogen bonding, dispersion forces, and hydrophobic effects between molecules.[8]

Electrostatic interactions (ion-ion, ion-dipole, and dipole-dipole) are attractions between opposite charges. Van der Waals forces, such as dispersion forces and dipole-

dipole interactions, are the weak forces between molecules arising from weak electronic coupling which act only over a very short distance. Hydrogen bonding consists of a hydrogen attached to an electronegative atom (oxygen or nitrogen) which gives a highly polarized bond, interacting with an electronegative atom in another molecule. The most important contributions to the complexation in aqueous solution are believed to originate from the hydrophobic effect, *i.e.* the penetration of the hydrophobic part of the guest molecule into the host cavity in aqueous solution.[9] A combination of these forces provides the enthalpic stabilization for the incorporation of the guest molecule within the host cavity,[10] and the stronger these forces are, the stronger will be the supramolecular complex.

The simplest example of supramolecular chemistry involves the minimum of two molecules to form what is known as a 1:1 host-guest inclusion complex, as described further on.[11] The host molecule is a large organic cage compound with an accessible internal cavity and the guest is a smaller molecule which can physically fit inside the host cavity. The driving forces for complexation are hydrophobic effects, lower enthalpy (intermolecular forces between host and guest), and higher entropy (release of solvent from host cavity and guest dissolution).[10] Inclusion into a host cavity can have significant effects on the guest including: 1) increased solubility, 2) increased stability, 3) increased fluorescence, 4) increased column retention and 5) modification of reactivity.[10] These effects on the guest have corresponding applications in everyday life: 1) drug delivery and the emulsification of food products, 2) storage of compounds, flavour enhancement in food products, 3) development of fluorescent sensors, 4) chromatography in columns and 5) hosts used as "nanoreactors" or "nanobeakers" for control of chemical reactions.[10] The formation of such

a complex is illustrated in Figure 4. This figure emphasizes that the formation of host-guest inclusion complexes in solution involves an equilibrium between the complex and the free guest and host molecules.

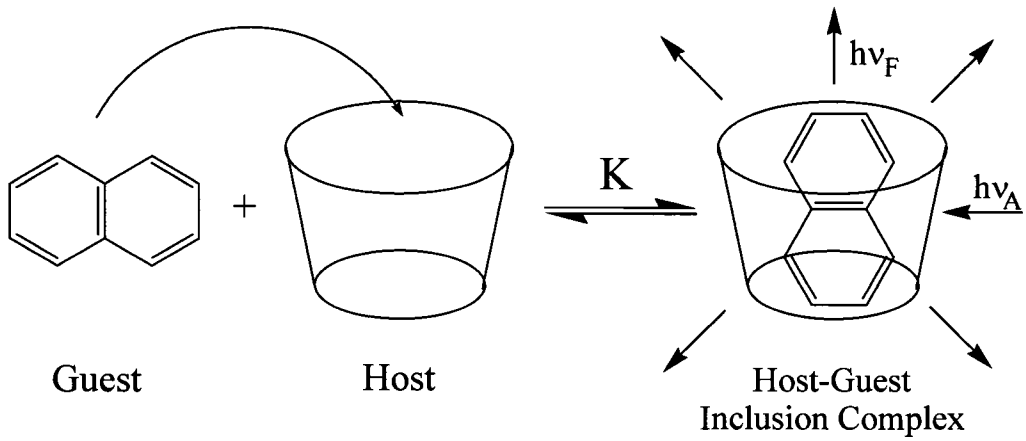

Figure 4 1:1 Host-guest inclusion complex

In this project, in order to study the host-guest interactions, and the physical and the spectroscopic properties of these supramolecular host-guest inclusion complexes, a steady-state fluorescence spectroscopy method is used. It allows for the measurement of the fluorescence spectrum of the host in the absence and presence of the guest, and from these the effect of complexation on the host fluorescence can be determined. One possible result of forming supramolecular complexes of guests within the fluorescent host is enhancement of the fluorescence intensity, as illustrated in Figure 4. This fluorescent enhancement, which will be explained in detail later in section I.3, is very easy to measure accurately as well as to relate to environmental changes of the probe (only true for guest fluorescence

enhancement), and thus provides an excellent method for studying the host-guest complexation process.[12]

Figure 4 shows the formation of a 1:1 host-guest complex, in which one guest molecule resides inside the cavity of the host molecule. It is also possible however, that higher order complexes can be formed. These include a 2:1 complex, in which two hosts cap the ends of a single guest molecule, a 1:2 complex in which two guests reside inside one host, or a 2:2 complex in which two hosts cap the ends of a pair of face-to-face guests. The analysis of the fluorescence spectra of the host molecule in the absence and presence of various amounts of the guest enables both the determination of the complex stoichiometry as well as the determination of the association constants for complexation. These association binding constants (K) are very important parameters which provide significant information on how well the host molecule accommodates the guest molecule into its internal cavity.

Furthermore, the temperature dependence of the complexation processes can also be studied, which allows for the determination of the two most fundamental thermodynamic quantities for the complexation process, namely the enthalpy and entropy. This provides for a better understanding of the forces responsible for the complexation of the guest molecule within the host.[12] Since the fluorescence lifetime is extremely sensitive to the guest environment, the investigation of the specific supramolecular host-guest systems by time-resolved spectroscopy can provide further useful insights into the interactions involved in host inclusion of a guest molecule.

I.2 *Fluorescence Spectroscopy*

The emission of light from any substance is called luminescence. This general term includes the specific processes fluorescence and phosphorescence.[12] Fluorescence refers to luminescence which involves a transition between states of the same multiplicity, whereas phosphorescence involves a transition between states of different multiplicities. It is also possible for transitions to occur non-radiatively (without the emission of a photon) through the release of excess energy as heat. Again, two distinct processes can be described: internal conversion (IC) and intersystem crossing (ISC). Internal conversion involves transitions between states of the same spin multiplicity, whereas, intersystem crossing involves transitions between states of different spin multiplicity.[12] These various transitions can be illustrated by a Jablonski Diagram, as shown in Figure 5.

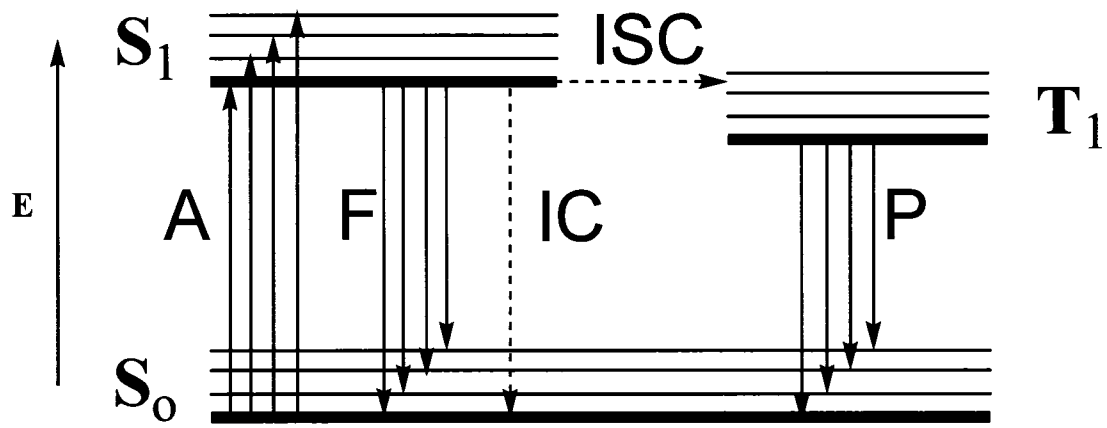

Figure 5 A simplified Jablonski diagram

The photophysical processes which occur upon absorption of a photon can be described as follows. In Figure 5 S_0, S_1 (and S_2) represent the electronic singlet states each containing vibrational energy levels (shown as equally spaced for convenience). When a molecule is in its ground state (S_o) it is in the lowest vibrational level and the higher vibrational energy levels are not generally populated at room temperature. The absorption of light energy ($h\nu_A$) happens within femtoseconds and the magnitude of this energy determines which S_1 (or S_2....) vibrational level becomes populated. The molecule relaxes to the lowest vibrational level of S_1 in the next few picoseconds; this process is called vibrational relaxation. The molecule is fully vibrationally relaxed at the time of emission which occurs on the order of nanoseconds from the lowest vibrational level. For this reason, the fluorescence spectrum is generally independent of the excitation wavelength.[13] The molecule returns to ground state after emission (fluorescence, k_f) or non-radiative (k_{nr}) relaxation. Thus, the process of fluorescence can be summarized by excitation, vibrational relaxation and emission.

The total fluorescence intensity I_F is related to the quantum yield (Φ_F), defined as the ratio of photons emitted to photons absorbed. From the Jablonski diagram it is obvious that there are two types of pathways to go from S_1 to the ground state (in the absence of quenchers), namely fluorescence and non-radiative decay. Φ can thus be expressed as the rate of photons emitted divided by the total rate of depopulation of the excited state:

$$\Phi_F = \frac{k_f}{(k_f + k_{nr})} \qquad (1)$$

The time dependence of fluorescence (for a homogenous sample of fluorophores) can be given by the equation:

$$I_F(t)=I_o\exp-\{t/\tau_F\} \qquad (2)$$

where τ_F is the reciprocal of the total first order rate constant, given as the sum of the first order rate constants for all depopulation processes:

$$\tau_F=\frac{1}{(k_f+k_{nr})} \qquad (3)$$

If the non-radiative relaxation is fast compared to fluorescence ($k_{nr}>k_f$), Φ_F will be small, that is the compound will exhibit very little fluorescence. The presence of quenchers (molecules which deactivate excited states) make non-radiative relaxation routes more favourable or provide additional non-radiative routes (such as energy or electron transfer) and often there is a simple relation between Φ_F and the quencher concentration. The best known quencher is probably O_2, which quenches almost all fluorophores. Other quenchers only quench a limited range of fluorophores.[14]

Phosphorescence on the other hand occurs by electrons relaxing from an excited triplet state to the ground singlet state by means of emitting a photon. In phosphorescence the triplet-singlet relaxation is spin forbidden resulting from differences in multiplicity between the two states, therefore phosphorescence is in general a much weaker phenomenon than fluorescence. Also, the lifetime of phosphorescence emissions (10^{-4} - 10^{2} s) is therefore

much longer than the lifetime of fluorescence emissions ($<10^{-6}$ s).[15]

A high quantum yield will result in brighter fluorescence , *i.e.* a high fluorescence intensity. As can be seen from Equation (1), the quantum yield can be close to unity if the rates of non-radiative processes are much smaller than the rate of radiative decay. Internal conversion often competes strongly with fluorescence, therefore, the rate of internal conversion is important when studying the quantum yield of a molecule. If the two electronic states are close in energy, the rate of internal conversion will be large. This is because it is easier to have a high vibrational level of the lower excited state at the same energy as the upper excited state, thereby allowing internal conversion to occur. If this is the case, the quantum yield will decrease, resulting directly in a decrease in fluorescence intensity. This phenomenon can be defined by the Energy Gap Law, which provides the relationship between the rate of internal conversion, k_{IC}, and the energy difference between the S_o and S_1, ΔE.[16] This relationship is given by the following equation:

$$k_{IC} \propto e^{-\Delta E/RT} \qquad (4)$$

In general, the excited state S_1 is more polar than the ground state, S_o, due to the promotion of an electron to the higher, larger, and more spread out molecular orbital. Therefore, the excited state molecule is more energetically stabilized relative to the ground state in a polar than in non-polar solvent (environment). This greater stabilization of the excited state in polar solvents decreases the energy gap between the S_o and S_1 states, and therefore, increases the rate of internal conversion. Transferring a molecule of interest from

a polar to a non-polar solvent or environment, the reverse phenomenon will occur. Destabilisation of the excited state will be observed, causing an increase in energy gap between the ground and excited states, as shown in Figure 6. This results in a decrease in k_{IC}, and thus an increase in quantum yield, ϕ_F, resulting in the observation of fluorescence enhancement.[16]

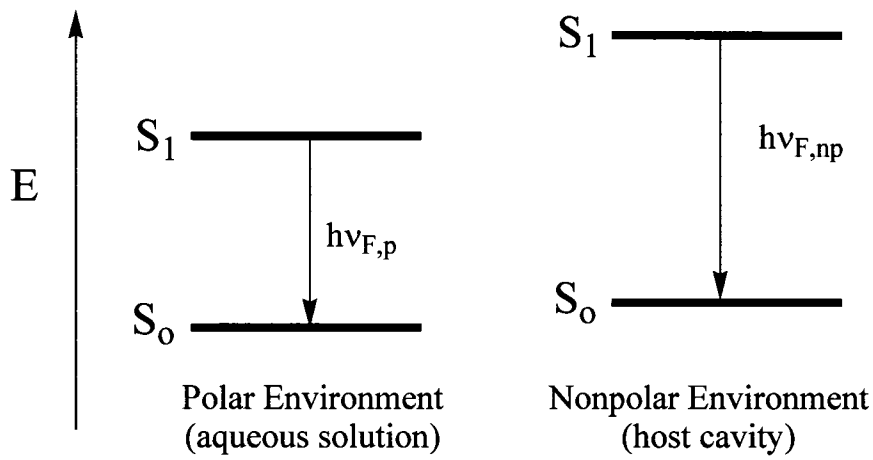

Figure 6 Polarity effects on guest fluorescence

The third very important property of molecular fluorescence is fluorescence wavelength maximum, λ_{Fmax}, which indicates the difference in energy between the lowest vibrational level of excited state and the most probable vibrational level of the ground state. Therefore, the change in energy gap between the ground and excited state will affect both the emission wavelength maximum and quantum yield. An increase in energy gap ΔE will

cause λ_{Fmax} to move to the shorter values of wavelength (higher energy) in the spectrum (blue-shift), since $\Delta E=hc/\lambda_F$.[16]

For many probes the values of k_{IC} and k_{ISC} depend on the fluorophore's environment in a way determined by properties such as refractive index, temperature and the local polarity. In this project, the polarity of the environment of the fluorescence probe is changed upon inclusion within a host. Since many fluorescent probes are hydrophobic, polar aqueous solution is a very unfavourable environment for them. However, if a host molecule that possesses a relatively non-polar cavity is added to the solution, the probe has the ability to become incorporated within the cavity, allowing the same probe to experience a completely different, more favourable environment.[16] This effect, namely the changing of the fluorescence properties of a guest molecule by changing its local environment upon inclusion inside the host cavities provides the means to study the supramolecular host-guest inclusion process.

The polarity effects discussed above refer to the enhancement of guests upon inclusion into hosts, which is not the main focus of the project, but is used occasionally. The main focus is in fact on the change in host fluorescence upon guest inclusion. In this case, polarity would not change much for a large host after including a small guest molecule. More likely there will be changes in the host configuration and electronic properties upon guest inclusion. This may lead to changes in electronic energy levels and the excited state of the host molecule. However, this would be very specific to each host-guest complex, and will be considered in the discussion section.

In the case of host fluorescence both enhancement and suppression have been

observed upon inclusion. The measurement of this fluorescence enhancement or suppression as a function of added guest concentration provides an accurate method for determining the value of the association constant K for the inclusion process, as described in Chapter I.3. In this project, two distinct types of fluorescence experiments were performed.

Steady-state fluorescence measurement is obtained when the sample is continuously irradiated by excitation light. This quickly establishes a steady-state population of the excited state, and thus a constant fluorescence emission intensity. This procedure can be used to measure the fluorescence spectrum of a compound, which is a plot of fluorescence intensity versus wavelength.[12] In this project numerous emission spectra were collected using a constant excitation wavelength in order to determine the relative fluorescence intensities at specific wavelengths for a sample.

Time resolved fluorescence involves the exposure of the compound to nanosecond flashes of light of a certain wavelength to prepare an initial population of the excited state, which subsequently relaxes. The intensity is then measured as a function of time (on the nanosecond timescale). This mode of fluorescence is used to determine the lifetime of a compound at a particular wavelength. The fluorescence lifetime of the excited state, τ_F, is the average time a molecule stays in the excited state before returning to ground state. This τ_F can be expressed as the inverse of the total depopulation rate, as shown previously in Equation 3. Typically fluorescence lifetime values are in the 1-100 ns range. Note that the expression for τ_F is related to the expression for Φ_F because they have a common denominator, and thus $\Phi_F = k_f\tau_F$.

I.3 *Determination of Association Constant (K)*

Fluorescence enhancement (or suppression) (F/F_o) is determined by dividing the integrated area under the fluorescence spectrum with guest present (the total fluorescence, F) by the integrated area under the host reference spectrum (F_o). The association constant, K, can be determined by fitting the "fluorescence titration" data, *i.e.* the plot of F/F_o versus [host] (for fluorescent guests) or [guest] (for fluorescent hosts). The following fluorescence titration fit equations were originally written for the case of non-fluorescent hosts and fluorescent guests. However, they can also be used in the situation where the host is fluorescent and the guest is non-fluorescent, as is the case in this project. In the case of enhancement (or suppression) of host (H) fluorescence upon addition of the non-fluorescent guest (G) the simplest case would be the formation of a 1:1 host-guest ({H:G}) inclusion complex. The measured enhancement (or suppression) depends on the added guest concentration according to the equation:[11]

$$F/F_o = \frac{1+(F_\infty/F_o-1)[H]K}{1+[H]K} \qquad (5)$$

where F is the integrated fluorescence intensity in the presence of the guest, F_o is the integrated fluorescence intensity in the absence of the guest, F_∞ is the integrated fluorescence intensity when all guest molecules have been complexed by host molecules[17] F_∞/F_o is the enhancement when 100% of the fluorescent host molecules are complexed, and K is the equilibrium binding constant for the 1:1 complexation, as given in the following equations:

$$H+G \rightleftharpoons \{H:G\} \quad (6)$$

$$K=\frac{[\{H:G\}]}{[H][G]} \quad (7)$$

The analogous equation applies for host fluorescence where the [H] in Equation 5 is replaced by [G].

Confirmation of 1:1 complexation can be obtained from the double reciprocal plot of $1/(F_\infty/F_o-1)$ versus 1/[H]; this will be linear if only 1:1 complexation is occurring but will be non-linear if higher-order complexes also form.[18] Thus, Equation 5 can be applied to the enhancement of the host fluorescence by added guest and can be used to determine the binding constant K from the fluorescence titration data of F/F_o for a fixed concentration of host as a function of guest concentration.

For 2:1 host-guest ({H:G}) complexation the binding equilibrium constants K_1 and K_2 can be defined as[19]:

$$H+G \rightleftharpoons \{H:G\} \quad (8)$$

$$K_1=\frac{[\{H:G\}]}{[H][G]} \quad (9)$$

$$\{H:G\}+H \rightleftharpoons \{(H)_2:G\} \quad (10)$$

$$K_2=\frac{[\{(H)_2:G\}]}{[\{H:G\}][H]} \quad (11)$$

The numerical values of K_1 and K_2 binding constants can be determined using the following equation:

$$F/F_o = \frac{1+F_aK_1[H]+F_bK_1K_2[H]^2}{1+K_1[H]+K_1K_2[H]^2} \qquad (12)$$

where $F_a=F_1/F_o$, $F_b=F_2/F_o$, F is the integrated fluorescence intensity in the presence of the guest, and F_o is the integrated fluorescence intensity in the absence of the guest molecule. In the case of host fluorescence, the analogous equation applies to a 1:2 host-guest complex where [H] in Equation 12 is replaced by [G].

The numerical values for the binding constants were determined using non-linear least-squares analysis programs, written by Dr. B.D. Wagner, based on Equations 5 and 12. In all cases, a total of 9-17 individual data pairs of (F/F_o, [G]) were analysed to obtain the value of K. Furthermore, at least three separate trials were performed, and the calculated K values were then used to plot the fitted curves of F/F_o vs. [G], and compared with experimental data.

I.4 *Thermodynamic Considerations*

The thermodynamic properties of the host-guest inclusion process can be determined using a number of different techniques, including microcalorimetry, electronic absorption, potentiometric techniques, and fluorescence spectroscopy.[12] In this project fluorescence spectroscopy is the chosen method of study. Association (equilibrium) constants (K) are

determined at various temperatures. These values can be used to determine the enthalpy change (ΔH °) and entropy change (ΔS °) of the inclusion process, using the following relationships:

$$\ln K = \frac{-\Delta G^{\circ}}{RT} \tag{13}$$

$$\Delta G^{\circ} = \Delta H^{0} - T\Delta S^{0} \tag{14}$$

Combination of Equations (13) and (14) gives the relationship between K, T, $\Delta H^0$and ΔS^0, which is known as the van't Hoff equation:

$$\ln K = \frac{-\Delta H^{0}}{RT} + \frac{\Delta S^{0}}{R} \tag{15}$$

ΔS^0, the standard entropy change, is a measure of the change in disorder of the system, and ΔH^0, the standard enthalpy change, is a measure of the energy changes associated with the complexation.

Equation (15) shows that a plot of lnK against 1/T will have a slope equal to $-\Delta H^0/R$ and intercept equal to $\Delta S^0/R$. If the plot of lnK against 1/T is linear, this means that ΔH^0 and ΔS^0 are independent of temperature over the range investigated. The importance of the van't Hoff equation lies in the fact that from the plot of lnK against 1/T, the two major thermodynamic quantities, enthalpy and entropy, can be determined giving further insight into the host-guest complexation, including which of the two dominates in the formation of

the supramolecular complexes.

I.5 *Detailed Description of the Three Host Molecules Studied*

In this project, the host molecules studied are methoxy nanoballs, cucurbit[6]uril analogues and bistren cages. All three of these host molecules exhibit fluorescent properties which is not the usual case studied by the Wagner group. The typical non-fluorescent host systems, such as cyclodextrins and cucurbit[n]urils, limit the host-guest studies to fluorescent guests. The new systems, made available with the fluorescent hosts, allow us to view the system from the perspective of host fluorescence and to use both non-fluorescent and fluorescent guests. This opens up whole new areas of research, and types of complexes. The host fluorescence can be studied in the presence of non-fluorescent guests or the guest fluorescence can be studied in an area where the host itself does not fluoresce. Due to the fluorescent properties of the host it may be possible to use them as fluorescent sensors for non-fluorescent guest molecules or to design nanomachines by forming extended host-guest systems which would have large fluorescent components. These three factors combined make these three hosts of particular interest and the basis of this project.

I.5.1 *Methoxy Nanoball*

The methoxy nanoball (MNB) as seen in Figure 1 represents a new extension of crystal engineering and coordination polymer chemistry. The basic unit used in the finite spherical structures (nanoballs) synthesized in this project, first synthesized by Zaworotko *et al.* [2,3], consist of two copper metal nodes connected by four bidentate isophthalic acid

ligands. In this case , the bidentate ligands used join the metal nodes at 120° angles yielding structures which close in on themselves.[2] This contrasts the infinite 2D sheets formed in coordination polymer chemistry when using ligands that join the metal centers at a 180° angle. This creates the four corners of the square molecular polygons which make up the small rhombihexahedron. (See Figure 7) This methoxy nanoball has a molecular mass of 6900 g/mol and molecular volume 11.5 nm^3. The structure is a structural isomer of the small rhombihexahedron with the methoxy moieties capable of coordinating to metal centers through their ether oxygen atoms to axial sites on adjacent nanoballs, which gives a double cross-linking.[3]

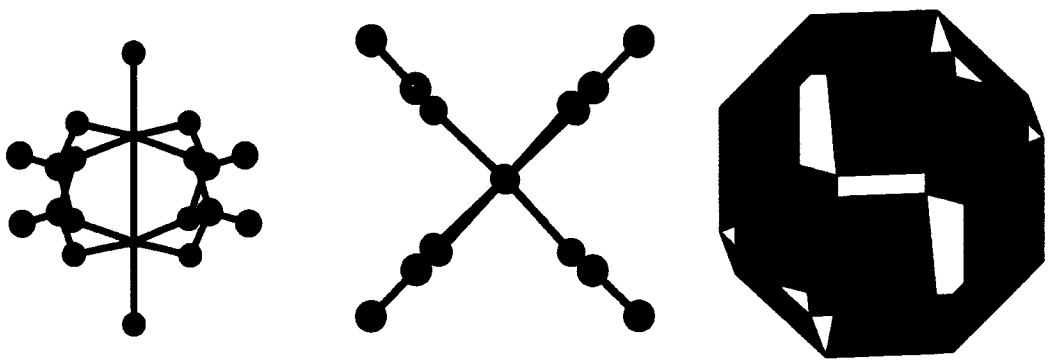

Figure 7 Basic unit for the nanoball synthesis

The nanoballs have the potential to be used as large discrete host molecules in solution. As mentioned previously, these structures have numerous shallow cavities on their surface, which may be sufficiently deep to allow for the complexation of guest species.

Furthermore, the interior is hollow, and may be accessible to small or narrow guests, as can be seen in Figure 1. As determined previously during my honours project work, not all nanoballs have fluorescent properties. Of the five nanoballs investigated (unsubstituted, methoxy, amino, sulfonato and nitro) only the methoxy nanoball exhibited any distinct fluorescence properties.[20] Therefore, the methoxy nanoball is the nanoball of interest for this masters project. In this project, the fluorescence and absorption studies of this host with various guests placed in the pits and hollows or the interior of the nanoballs will be investigated to ascertain potential of these nanoballs as hosts and therefore fluorescent sensors.

I.5.2 *Cucurbit[6]uril Analogue*

Cucurbit[n]urils are a group of cyclic oligomeric molecules named for their perceived resemblance to pumpkins, *i.e.* members of the cucurbitaceae family, as seen in Figure 2.[21] The groups of Mock[22-25], Buschmann[26,27], and Kim[28-30], have defined the molecular recognition properties of CB[6] itself (the original cucurbituril) and have demonstrated its application in self-assembly studies after the elucidation of the molecular structure by Mock in 1981. CB[6] has the ability to encapsulate several different types of guests in its hydrophobic cavity because of a combination of noncovalent interactions including the hydrophobic effect, ion-dipole interactions, and hydrogen bonding. The selectivity of CB[6] is due to the rigidity of the macrocycle which allows for guests of proper size, shape and functionality to form thermodynamically stable complexes.

The observation of CB[6] encapsulating guests was first reported using alkyl

ammonium ions on the basis of experimental data from ^{1}H NMR[31], UV-vis[32], and calorimetry.[33] Since then, the binding of CB[6] to alkali metal cations[34], amino acids, amino alcohols[35], and amino azabenzenes[36] has been reported. In contrast a limited number of investigators have used fluorescence experiments to determine the binding constants of certain guests towards CB[6]. Because CB[6] is not fluorescent, these studies from the groups of Wagner[37-40], Kim[41,42], Buschmann[43] and Nau[44] employ fluorescent guests.

The further development of CB[6] supramolecular chemistry requires tailor-made synthetic approaches that provide control over size, functionalization pattern and solubility characteristics of the formed CB[6] derivatives. Recently a new class of macrocyclic hosts, CB[6] analogues, was reported which are based on glycoluril and bis-phthalhydrazide.[45] The recognition properties of these CB[6] analogues differ from those of CB[6] because two aromatic walls have been incorporated into the macrocycle which (1) defines a cavity lined by aromatic rings which should impart a high selectivity for aromatic and cationic guests, (2) allows for detection by UV-vis and (3) allows for detection by fluorescence.[46] In the particular CB[6] analogue used in this project the glycoluril R substituents are CO_2H groups (see Figure 2) and its molecular recognition properties are obtained using fluorescence spectroscopy. This CB[6] analogue is also referred to as LB[6] because it was unofficially named after its creator, Jason Lagona (a graduate student in the Isaacs group at the University of Maryland with whom our group collaborates), and the LB[6] is short for Lagonabit[6]uril.

The incorporation of the phthalhydrazide walls into the macrocycle provides the opportunity for detection by long wavelength UV-vis and fluorescence spectroscopy (see

Figure 2). In addition to ion-dipole interactions and the hydrophobic effect, complexes of the CB[6] analogue also benefit from π-π interactions with guests containing aromatic rings. Aside from the different chemical functionality of the walls of the CB[6] analogue relative to CB[6], the CB[6] analogue also possesses a very different shape from CB[6] itself. Its cavity is oval as opposed to spherical, which imparts selectivity for longer, flatter aromatic guests relative to CB[6] which prefers more spherical guests.

This fluorescent host was studied previously by the Wagner group with both benzene and Nile Red as guests.[46] Benzene formed a 1:1 complex with LB[6] exhibiting fluorescence enhancement; while Nile Red gave a 2:1 complex with fluorescence suppression. Therefore, this host shows potential for further host-guest studies, which were undertaken in this project.

I.5.3 *Bistren Cage*

Bistren cages were first designed to host polyatomic anions, in particular those having a rodlike shape.[47] In order to provide electrostatic binding, some amine groups of the cage have to be protonated and the selectivity of the receptor-substrate interactions depends on the matching of the length of the anion with that of the cavity.[47] Bistren cages have also been designed to host pairs of transition metal ions, each metal occupying a tetramine compartment. Given the stereochemical arrangement imposed by each tren subunit, a trigonal bipyramidal structure can be assumed, with one of the axial positions of the bipyramid exposed to the coordination of a further ligand. Thus, ambidentate polyatomic anions can bridge the two metal centers, giving rise to a stable adduct.[12]

The amine groups as shown in Figure 3 are efficient electron transfer quenchers of anthracene fluorescence.[12] At low pH, the amine groups are protonated to the ammonium form, which does not quench anthracene fluorescence and the cage is highly fluorescent. At a high enough pH so that at least one adjacent nitrogen is in the amine form, the fluorescence is efficiently quenched. This is illustrated in Figure 8, which shows the pH dependence of the fluorescence of this cage (o). In the presence of two equivalents of Zn(II), however, the Zn cations enter the cage and engage the amines, greatly reducing the amine quenching and restoring the cage fluorescence. This is also shown in Figure 8 (▽). Thus at pH 8.5, the dizinc (II) cage is fluorescent. This fluorescence can still be quenched, however by the presence of certain anions, such as N^-_3, which can enter the cage and cause a photoinduced electron transfer quenching process to occur, as shown in Figure 8 (◇). The authors propose this dizinc (II) cage as an efficient and highly selective sensor for ambidentate anions.[12]

This particular host has huge potential for the Wagner group because it has been virtually unexplored as a fluorescent host. There has been only one paper written using this host[7]. In that case it was used to detect anions, not organic guests as studied in this thesis. In this project, the broader host capabilities of this bistren cage were explored, using a series of substituted benzenes as simple aromatic, neutral guests.

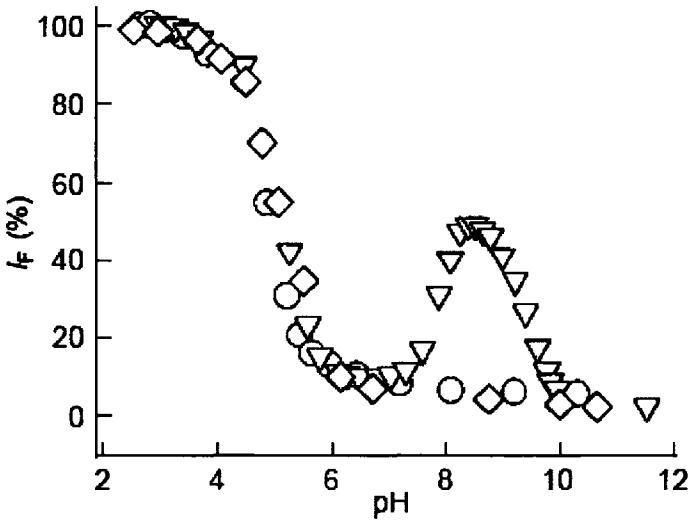

Figure 8 pH dependent fluorescence of bistren cage

(Reproduced from reference 7)

I.6 *Guest Molecules Used*

The guests molecules which are used in this project to study host-guest inclusion complexes with the three hosts are numerous aromatic molecules, all of which are listed in the respective host results and discussion sections. The smallest aromatic guest (benzene) was tried first as a basis point for further experiments. Since one goal of this project was to attempt the formation of nanomachines, switches or sensors, the other guests chosen were also aromatic but longer and hence capable of being complexed by two hosts. Therefore, it may be possible to join two host molecules together to form the desired complexes. These other aromatic guests were longer due to additional aromatic segments and/or substituents in the backbone or appendant arms which may also aid in complex formation.

II. *EXPERIMENTAL*

II.1 *Chemical Sources*

The chemicals used for this project and their sources are listed in Table 1. All were used as received.

Chemicals	**Manufacturer, Purity**
methanol	Aldrich, 99.9% ACS spec grade
5-methoxyisophthalic acid	Aldrich, 97%
2,6-lutidine	Aldrich, 99%
copper (II) nitrate hemipentahydrate	Aldrich, 98%
nitrobenzene	Fisher, Certified
LB[6]	Received from Dr. Lyle Isaacs, University of Maryland
9,10-bis(chloromethyl)anthracene	ABCR GmbH & Co. KG
tris(2-aminoethyl)amine	Aldrich, 96%
toluene	Aldrich
terephthaldicarboxaldehyde	Aldrich, 99%
sodium borohydride	Aldrich, Reagent Plus 99%
dichloromethane	Aldrich, 99.6% ACS reagent
sodium sulfate	Aldrich, ≥99.0%, ACS reagent
benzene	BDH Chemicals, glass distilled
Nile Red	Aldrich
curcumin	Aldrich
toluene	BDH

Chemicals	Manufacturer, Purity
pyridine	Fisher
biphenyl	Eastman
2,6-ANS	Molecular Probes
1,8-ANS	Aldrich
2,6-TNS	Molecular Probes
4,4'-dipyridyl	Aldrich, 98%
m-phenylenediamine	ICN
p-nitrophenol	BDH
hydroquinone	Baker
benzoic acid	Anachemia
phenol	Baker
xanthone	Aldrich, 97%
catechol	Fisher
resorcinol	BDH
naphthalene	Fisher, Purified
anthracene	Eastman
pyrene	Aldrich, 99%
nitrobenzene	Fisher, Purified
aniline	Fisher
chlorobenzene	Fisher
l-tyrosine	BDH/VWR
guanine	Aldrich
o-phenylenediamine	Anachemia
β-cyclodextrin	Aldrich
HP-β-cyclodextrin	Aldrich

Chemicals	Manufacturer, Purity
γ-cyclodextrin	Aldrich
HP-γ-cyclodextrin	Aldrich

Table 1 List of chemicals used for this project

II.2 *Synthesis of Host Compounds*

II.2.1 *Methoxy Nanoball*

The methoxy nanoball was synthesized using a layering method to allow crystal formation over time, according to the methodology supplied by Dr. Michael Zaworotko from the University of South Florida.[3] The procedure and chemicals used for the synthesis are summarized below and in Table 1.

Procedure: Green crystals were formed by layering a methanolic solution (3.0 mL) of 5-methoxy isophthalic acid (20 mg, 0.10 mmol) and 2,6-lutidine (0.035 mL, 0.30 mmol) onto a (3.0 mL) methanolic solution of copper (II) nitrate hemipentahydrate (23 mg, 0.099 mmol) which contained nitrobenzene (1.0 mL) as templates. Green crystals were formed within a day.

The MNB has molecular formula $[Cu_2(5\text{-MeO-bdc})_2(MeOH)_x(H_2O)_{1.83-x}]_{12}$ and a diameter of 2.8 nm.[3] The crystals were kept in the vial in the mother liquor for storage and were removed from the vial with a spatula and dried on filter paper before use.

II.2.2 *LB[6]*

The synthesis of LB[6] is described in the literature.[45,48-49] After discussing the extensive procedure it was realized that there were too many potentially dangerous chemicals and steps involved in this procedure that our lab was not equipped for or prepared to undertake, especially considering the low reported yield. Thus, we worked with a small amount of sample provided by Isaacs' group.

II.2.3 *Bistren Cage*

The octamine starting material was prepared as follows: 9,10-bis(chloromethyl)anthracene (1.5g, 5.4mmol) and tris(2-aminoethyl)amine (tren, 4.73g, 32.4 mmol) were dissolved in toluene (50mL) and the solution was refluxed with magnetic stirring for 6 hours. After being cooled to room temperature, the resulting yellow-orange solution was filtered, then the solvent and the excess tren were distilled off at reduced pressure, giving the octamine as an orange oil.[50]

A solution of terephthalaldehyde (4.0 mmol in 250 mL methanol) was added dropwise over 2 hours under magnetic stirring to a solution of bistren derivative of the 9,10-anthracenyl fragment (2.0 mmol in 750 mL methanol). The stirred solution was then heated to 50°C and 2.5 grams of sodium borohydride was added in small portions over 3 hours. The solution was then stirred overnight at room temperature. Methanol was distilled off under reduced pressure, and the residue was dissolved in 100 mL of water. The aqueous solution was extracted with dichloromethane (3x50mL). The organic phase was dried over sodium sulfate and the solvent was removed under reduced pressure to give a gold-yellow

solid.[7] The characterization of this compound is outlined in section II.12.

II.3 *Sample Preparation*

In this project similar experimental methods were used for preparing the solutions with respect to the three different host molecules used.

Before absorption and fluorescence analyses could be performed the solubility of MNB was investigated to find the best solvent in which to dissolve the host. The MNB was most soluble in a phosphate buffer of pH 6.80 created by dissolving 8.44 g potassium monobasic phosphate and 6.60 g of potassium dibasic phosphate in 1000 mL of deionized water. The pH was measured to be 6.80 using an Accumet pH meter 910.

The LB[6] host was previously determined to be most soluble in acetate buffer.[46] The acetate buffer used had a pH of 3.50 and was made by dissolving 3.00 g of acetic acid and 4.10 g of sodium acetate in 1000 mL of deionized water.

Although the bistren cage was soluble in both the phosphate and acetate buffers described above it had the highest solubility in water. Therefore, all samples prepared for fluorescence measurements were done in water which is an easier medium with which to work.

The various solutions of MNB were prepared for analysis in the following manner: a small quantity of solid nanoball was removed from the mother liquor in the vial and allowed to dry on filter paper. The dried nanoball was then dissolved in approximately 3 mL of the appropriate solvent (phosphate buffer or water) in a small sample vial, with dissolution aided using a sonicator. The solution was then filtered through a Kimwipe in

a pipette into a 1 cm^2 quartz cuvette.

LB[6] and bistren solutions were made up to the appropriate concentration in the appropriate solvent using a sonicator to aid with dissolution.

II.4 *UV-Vis Absorption*

All absorption measurements were performed on a Cary 50 Bio UV-Visible spectrophotometer.

For each host sample, the 1cm^2 quartz cuvette was placed in the spectrophotometer sample chamber and the scan was run from 250-600 nm using medium scan rate. The resulting absorption spectra were analysed to determine the wavelength of maximum absorption, which was used to determine appropriate fluorescence excitation wavelength.

II.5 *Steady-State Fluorescence*

Steady-state fluorescence measurements were performed on an LS 55 Perkin Elmer luminescence spectrometer. The solutions for each host were prepared in the same way as for the absorption measurements but the concentration of the solutions were changed accordingly so that the absorption at the excitation wavelength was between 0.25 and 0.35. This range of absorption is optimum for obtaining the best fluorescence spectrum.[12] The cuvette was then placed in the sample chamber of the fluorimeter and the excitation and emission slits were adjusted to allow an optimal amount of light to hit the cuvette and the photomultiplier tube. The excitation wavelength chosen was usually that of maximum absorption, and the emission wavelength range was chosen to start at approximately 10 nm

above the excitation wavelength and end at approximately 600 nm. These conditions were used if the host fluorescence was being studied. However, if the guest fluorescence was being examined, as in the case of curcumin and 1,8-ANS with LB[6], the excitation wavelength and emission range were chosen according to their respective maximum absorption wavelengths.

For the methoxy nanoball, the excitation wavelength was chosen as the wavelength of maximum absorbance, namely 290 nm. The emission wavelength range was chosen from 300-600 nm with a scan rate of 120 nm/min and the excitation and emission band widths set accordingly (usually 10.0 nm and 15.0 nm respectively).

The excitation wavelength used for LB[6] was 337 nm for host fluorescence and 425 nm for guest fluorescence. The corresponding emission range was from 347 nm (450 nm) to 770 nm (700 nm) and the scan rate was again 120 nm/min with the band width set at 15.0 nm for excitation and 10.0 nm for emission.

The bistren host required the excitation wavelength to be 340 nm with emission from 350-600 nm. The scan rate was the same as for the other two hosts and the excitation and emission band widths were usually set at 15.0 nm and 2.5 nm respectively.

The resulting fluorescence spectra were analysed to determine wavelengths of maximum fluorescence intensity ($\lambda_{F,max}$), total intensity (I_F) and integrated area (F) which can be used to determine physical and chemical properties of the molecule being studied. For each scan performed, a scan of the solvent used was measured and subtracted from the spectrum of the sample to eliminate any contribution from the solvent.

II.6 *Host-Guest Fluorescence*

A fluorescence titration involves measuring the fluorescence spectrum of the fluorescent host alone, and then in the presence of varying concentrations of the guest molecule. The resulting effect on the fluorescence can then be examined to determine if a complex has been formed and what type of complex it is. Some examples of the various guest molecules used can be seen in Figure 9 below.

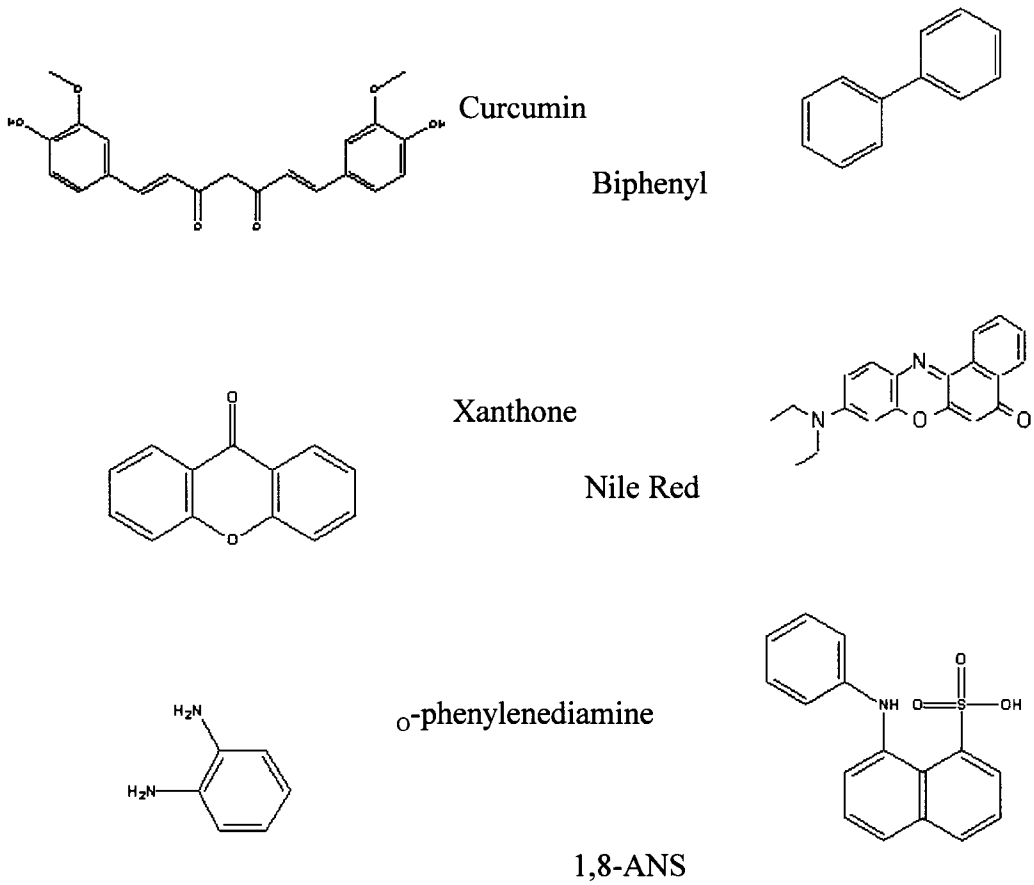

Figure 9 Guests used for inclusion studies

In the case of the experiments where the nanoball fluorescence was being investigated as a function of added guest molecule, a solution of host was prepared in the appropriate solvent using the same method as for fluorescence measurements. A scan was done on the host itself as a reference solution. Then solutions of various concentrations of guest in the presence of a fixed concentration of host were made by using one 2.5 mL solution of the highest concentration to be studied and making dilutions to it with the stock host solution. The cuvettes were then inverted several times to allow for adequate mixing of host and guest before fluorescence measurements were conducted. As always a baseline scan of the solvent was performed and subtracted from all scans done for accuracy. The resulting spectra were integrated and the fluorescence enhancement was determined. This quantity was subsequently used in 1:1 and 1:2 (host:guest) fit equations in order to determine the stoichiometry and binding constants of the particular host-guest complex created.

In the case of the experiments where the fluorescence of the guest was being investigated as it was incorporated into the host, a saturated bulk solution of guest was prepared in the appropriate solvent using the same methods as for fluorescent measurements. Then solutions of various concentrations of host were made by making dilutions with the stock guest solution to the highest concentration of host made. The blank, solvent and various host concentrations were all scanned and analysed in the same manner as mentioned above for host fluorescence. The F/F_o values obtained in these cases can also be used to help determine the fit of the host-guest complex.

LB[6] was also studied with the fluorescent guest curcumin using both guest and

host fluorescence. For the first case where the effect of LB[6] on curcumin fluorescence was studied six trials were performed and are outlined below, in each case the samples were diluted with the curcumin solution.

Trial one involved making up a 25 μM LB[6] solution in only 5 mL of filtered, saturated curcumin in acetate buffer which used only 0.0002 g of LB[6]. This 25 μM solution was titrated by decreasing the concentration by half each time from 25 μM to 0.78 μM. In the second trial a larger amount of LB[6] was used (0.0012 g) to make the 25 μM solution for titration. Again the concentration was diluted by half from 25 μM down to 0.78 μM. A third trial was done to try and achieve reproducible results. This time a 25 μM solution of LB[6] in acetate buffer was made for comparison and scanned under the same concentration reductions from 25 μM to 0.39 μM. Trials 4,5 and 6 were all done under the same conditions but dilutions of a quarter were made each time from 25 μM to 0.33 μM to obtain more data points for analysis.

From the other point of view, looking at how the curcumin affects the LB[6] fluorescence, several trials were also performed. The curcumin solutions were made up in acetate buffer and needed to be saturated due to solubility issues. Three trials were done by starting with the saturated solution and doing dilutions of a quarter each time by adding LB[6] solution to see the effect on the LB[6] fluorescence. The concentration of the saturated curcumin solution was determined by preparing a 2.5×10^{-4} M curcumin solution in 50 mL of methanol, in which curcumin is soluble. After the solution sat overnight 12 μL of this solution was added to 25 mL of acetate buffer to make a 2.0×10^{-8} M solution of curcumin in acetate buffer. Then a saturated curcumin solution was made in acetate buffer

for comparison and it too was left overnight and then filtered.

The effect of LB[6] on the fluorescence of 1,8-ANS was also examined. In order to do this a 10 μM 1,8-ANS solution was made in acetate buffer and half of this was used to made a 25 μM LB[6] solution and titration dilutions were made by 750 μL each time with the 1,8-ANS acetate buffer solution.

All bistren inclusion experiments were done to study the effects of guests on the host fluorescence. In each case a stock solution of host was made up to approximately 0.02 mM in 50 mL of deionized water. This stock solution was used to make the solutions of various guest concentrations to perform a fluorescence titration. In the cases where the guests were liquid, injections of the guest were made to the same 2.5 mL host solution using a 10 μL syringe for increasing guest concentration. Guests which were in the solid form were weighed into separate vials for the higher concentrations with 2.5 mL of host solution and sonicated to aid with dissolution. For the lower concentrations, the higher concentration solutions were diluted by half using the stock host solution. As with the previous two hosts, a blank was scanned with just the host present as a reference and a solvent blank was measured and subtracted from all fluorescence spectra. All solutions were transferred to cuvettes which were inverted several times to aid in host-guest mixing before measurements were performed. The areas under all the fluorescence curves were determined and used to calculate F/F_o values which were then used to determine the type of host-guest complex formation (1:1 or 1:2). These fits helped determine the binding constant values which were used to develop a trend in guest binding.

II.7 *pH Dependence*

To help determine the pH dependence of the methoxy nanoball fluorescence a 25 mL solution of MNB was made in acetate buffer and the fluorescence was tested. The solution was then transferred to a 50 mL beaker and the pH was increased by approximately 0.5 pH units each time by adding sodium acetate to the solution while being stirred on a stir plate and monitoring with a Accumet pH meter 910. The pH meter was calibrated with both a pH 7 and a pH 3 standardized buffer solution before measurements were taken to ensure accuracy. The fluorescence was retested again after each pH adjustment. For the higher pH range a 25 mL solution of MNB was made in phosphate buffer and the fluorescence tested. Again the solution was then transferred to a 50 mL beaker but this time the pH was increased by adding potassium dibasic phosphate at approximately 0.5 pH units each time while stirring the solution and monitoring the change with a pH meter. Between pH adjustments the fluorescence was retested to check for a pattern.

II.8 *Thermodynamics*

The temperature of the sample in the fluorimeter was controlled using a Fischer Scientific Isotemp 1016 temperature control bath. The temperatures used were 8 and 32 °C for methoxy nanoball and benzene in phosphate buffer. In all cases, at least three trials for each set of data were collected at the above mentioned temperatures. The concentrations of methoxy nanoball ranged from 0 mM to 40 mM. The spectrum of each nanoball: benzene system was collected, both in the absence and presence of benzene molecules. For each set of spectra, the fluorescence enhancement factors, F/F_o, were then calculated at the

various concentrations of the guest molecule, benzene. The association constant, K_1 was determined using the computer program to fit fluorescence enhancement vs. benzene concentration data to the 1:1 host-guest complex (Equation 5), using non-linear regression techniques. The values for these constants were then averaged between the appropriate trials for given temperatures.

A limited supply of LB[6] was available, so only one trial was performed at each of the following temperatures: 8, 15 and 32°C and three trials had previously been performed at 22°C.[46] The titrations were done from 0 mM to 40 mM benzene present in acetate buffer. As with the nanoball, the F/F_0 values were determined for each temperature and were used in the 1:1 computer fit program to establish the K values.

Thermodynamic studies were also performed on the bistren host, both with anisole and phenol as guests in water. In both cases one trial was performed at 8 and 32°C and three trials had previously been performed at 22°C. For the anisole trials the concentrations ranged from 0 mM to 40 mM anisole present. As for the phenol titrations the guest concentration ranged from 0 mM to 20 mM. These titrations were then analysed to determined the F/F_0 values which were entered this time into the 1:2 computer fit program based on Equation (12). This fit was used to establish both the K_1 and K_2 values which were then compared for each temperature.

II.9 *Time-Resolved Fluorescence*

Time-resolved fluorescence measurements were performed on a Photon Technology International Time Master fluorescence lifetime spectrometer. This instrument uses the

stroboscopic method of fluorescence decay curve measurement. The solutions were prepared in the same way as for the steady-state measurements. The cuvette was then placed in the sample chamber of the time-resolved fluorimeter and the band-passes were fully opened to allow maximum light to hit the sample due to the weak nature of the bands examined. The excitation wavelength chosen was the same excitation wavelength used for steady-state fluorescence. The emission wavelength chosen was that of maximum fluorescence intensity for that particular peak in the steady-state fluorescence spectrum. The resulting fluorescence decay curves were analysed using the non-linear least squares program (part of the instrument software) to determine the lifetime of each peak and the χ^2 value for the fit. The scatterer excitation (see below) was always set at the same wavelength as the sample excitation and the start and end delays for each scan were always set at 40 ns and 110 ns respectively.

In each case, a scan was done on the sample solution as it was prepared (unpurged) and then after the oxygen was replaced with argon (purged) to determine the effects of oxygen as a quencher on the various solutions and peaks. In order to purge a solution with argon a long necked 1 cm^2 quartz cuvette was used. A rubber septum was placed over the neck of the cuvette and a bleeder needle was placed in the septum to allow the oxygen to escape. A needle clamped to a hose for connection to the argon tank was then inserted all the way to the bottom of the cuvette. The argon gas was turned on and bubbled through the solution for approximately five minutes to purge to oxygen before taking the time-resolved fluorescent measurements.

Emission wavelengths of 330 nm and 448 nm were used for MNB itself and with

40 mM benzene present, with excitation at 290 nm in both cases.

The LB[6] system was analysed with both 0 mM and 10 mM benzene present. The excitation wavelength used was 360 nm whereas emission was set at 510 nm.

Bistren was also analysed for lifetime values, this time with 0, 10, 20, 30 and 40 mM aniline present. Excitation wavelength was set at 340 nm and the emission wavelength was 425 nm.

The decays were analysed by one, two and three exponential fit analysis using the software available with the instrument. The software can fit up to four exponential decays, and uses the fitting law:

$$I_F(t)=\sum a_i e^{-t/\tau} \qquad (16)$$

where a_i is the preexponential factor and $I_F(t)$ is the fluorescence decay curve. The preexponential factor assigned to a lifetime is a mathematical weighting factor for that lifetime value in the overall fluorescence decay. The χ^2 value is an indication of how good the exponential fit is to the actual decay. The closer its value is to unity, the better is the fit to the actual fluorescence decay.

The time-resolved fluorescence fit and deconvolution process is based on the instrument lamp profile. If the excitation was instantaneous, *i.e.* the lamp profile was infinitely narrow, then all molecules would be excited at the same time and relax together. Therefore the graph of the natural log of the data would be a straight line. However, the lamp profile is 1-2 ns wide so some molecules are excited at the beginning of the profile and

some at the end which gives a broad curved graph. In order to deconvolute the graph the lamp profile is measured using a colloidal silica scatterer solution (with similar intensity as the sample) to measure the lamp profile. This lamp profile is used to generate a calculated decay curve to compare to the sample decay curve once it is measured. When the spectrum is deconvoluted, then it can be fit using the Time Master software and the lifetime and chi squared values can be determined.

II.10 *Synthesis of MNB with Encapsulated Guests*

An attempt was made to incorporate the guest naphthalene into the nanoball structure during its synthesis. A 0.10 mM addition of naphthalene was made to the bottom layer of the nanoball system which resulted in a darker green solution than usual. The solution was allowed to sit over the weekend during which time crystals formed. A saturated solution of the naphthalene-nanoball crystals was made in 3 mL of phosphate buffer and was sonicated and filtered before testing the absorbance. A similar attempt was made to include pyrene in the MNB structure. This was done again by adding 0.10 mM of pyrene to the bottom layer of the nanoball system which resulted in a brighter green solution than usual. The solution was treated the same as the naphthalene-nanoball solution. A final attempt was made for encapsulating a guest, this time with Nile Red. With Nile Red a 0.10 mM addition was made again to the bottom layer of the nanoball resulting in a purple solution and purple crystals being formed over time. The solution was made in phosphate buffer and treated as before.

II.11 *MNB as a Guest*

Attempts were made to include the methoxy nanoball as the guest into four different cyclodextrin host molecules: β-CD, HP-β-CD, γ-CD and HP-γ-CD. A MNB solution was made up in phosphate buffer and then 3 mL of it was put in each of four different sample vials. An appropriate amount of each cyclodextrin was then added to a separate vial each to make up 10 mM solutions. Absorption and fluorescence spectra were measured to see if they had any effect when compared to the isolated MNB spectra. These same cyclodextrin solutions were also prepared in just phosphate buffer in the absence of MNB for comparison.

II. 12 *Bistren Characterization*

The structural characterization of the bistren host was done using both NMR and HPLC. The NMR samples were made by dissolving the largest amount of bistren possible in both $CDCl_3$ and D_2O forming saturated solutions. The bistren was more soluble in the D_2O so 1 mL of this solvent was used to dissolve the bistren. The solution was then transferred to an NMR tube which was then tested using standard NMR techniques on a Bruker 300 MHz NMR with XWIN NMR processing software.

A Zorax RX C18 column was used accompanied by a reverse phase guard column. The mobile phase was a 50%-50% gradient of methanol and water. The HPLC used consisted of a Perkin Elmer Binary LC Pump 250, Peak Simple Chromatography Data System SRI Model 203 Single Channel Serial Port, an Applied Biosystems 783 A Programmable Absorbance Detector and Peak Simple software. The method used for

detection consisted of changing the methanol-water gradient over time. The gradient was 50%-50% for 30 minutes the 100%-0% for 15 minutes and then 50%-50% for the remaining 5 minutes.

The bistren sample was made by dissolving 0.0069 g in 250 μL methanol + 100 μL water giving a total 350μL solution of which 20μL was used for injection. This injection was made into the sample loop and column of the HPLC and was analysed using standard methods. The peaks of the chromatogram were collected in vials as they eluted from the column and were further analysed.

III. *Results and Discussion: Methoxy Nanoball*

There were several different methods used to investigate the physical and supramolecular properties of the methoxy nanoball (MNB) and they are outlined in the following sections of this chapter. These spectroscopic methods helped determine the fluorescent and host properties of the nanoball. Once these properties were established they were then used to help design specific host-guest complexes. These complexes were then studied using the host fluorescence; this illustrates the unique aspect of this project.

III.1 *UV-Vis Absorption*

The absorption spectra of the MNB and the corresponding 5-methoxyisophthalic acid (5-MIA) ligand were acquired and compared as shown in Figure 10. As reported in my honours thesis [20] it was clear from the absorption spectrum that the nanoball absorption consists of a main peak at 260 nm unique to the nanoball and a shoulder around 290 nm which is similar to the ligand absorption. Thus, the electronic states of the nanoball are different from those of the ligand, indicating interactions between the ligand and metal.

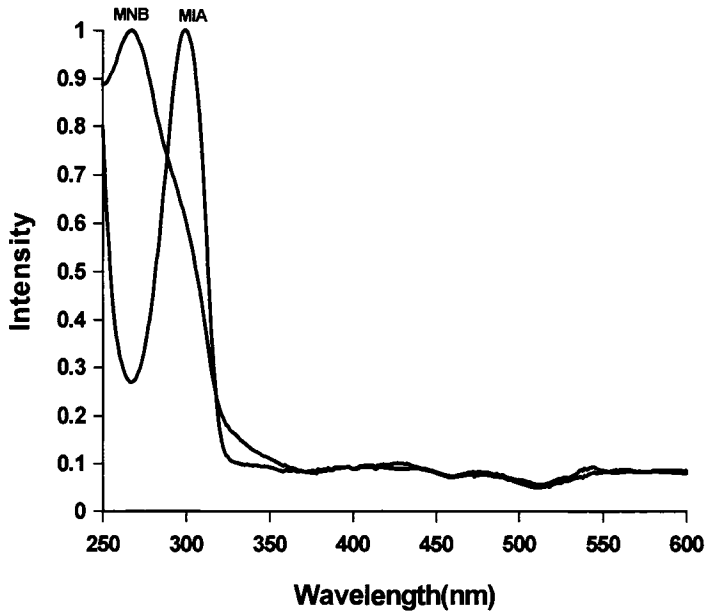

Figure 10 Absorption spectra of MNB and 5-MIA in phosphate buffer

III.2 *Steady-State Fluorescence*

The contribution of the 5-MIA ligand toward the overall MNB absorbance was confirmed with steady-state fluorescence investigations. As seen in Figure 11 the nanoball fluorescence spectrum (λ_{ex}=290 nm) consists of a strong band at 330 nm, and weaker bands at both 448 nm and 670 nm. However, when compared to the fluorescence spectrum of the 5-methoxy isophthalic acid ligand it is clear that both the first and third bands arise from the ligand itself and are therefore referred to as ligand centered bands.[51] This figure also shows that the band at 448 nm arises from the overall nanoball structure, involving charge-transfer interactions between the ligand and metal centres; either ligand-to-metal charge transfer (LMCT) or metal-to-ligand charge transfer (MLCT).

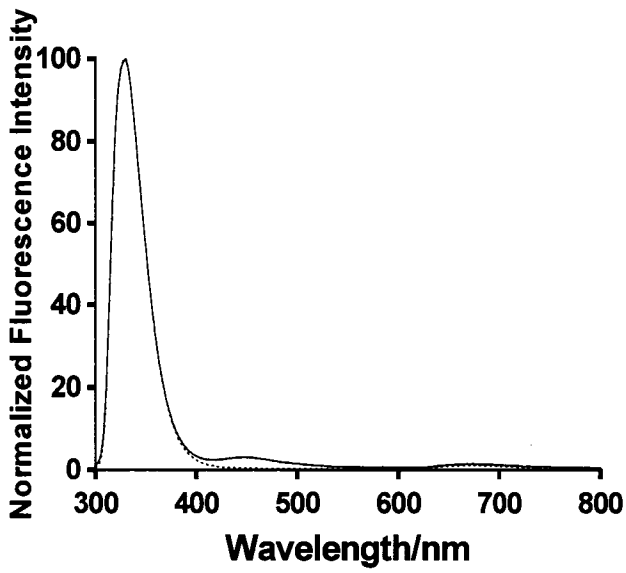

Figure 11 Fluorescence spectra of — MNB and ...5-MIA in phosphate buffer

It is proposed that the second band is a ligand-to-metal charge transfer (LMCT) band. This is based on the literature describing such bands. One article describes Cu(II) LMCT absorption spectra as having maximum absorption around 245 nm which is similar to the MNB value of 260 nm.[52] Another paper using Cu(II) compounds describes the fluorescence spectrum as having a band around 395 nm which is also consistent with the MNB spectrum.[53]

By comparison an article reviewing metal-to-ligand charge transfer (MLCT) stated that there would be a red shift in absorption peaks from the ligand spectrum compared to the metal-ligand spectrum.[54] The absorption spectra of MNB and 5-MIA are shown in Figure 10; this clearly shows a blue shift in this case from 299 nm to 267 nm. This

suggests that this is not a MLCT band. Another experiment was carried out to determine whether this band was present in a solution of the free metal and ligand or whether it was indeed do to the overall nanoball structure. A solution of the 5-MIA ligand was made in phosphate buffer and the fluorescence scanned. Then a small amount of copper(II)nitrate hemipentahydrate was added to see if the peak appeared at 448 nm. However, the peak at 448 nm did not appear (see Figure 12). This lead to the conclusion that the peak must be due to the electronics of the entire nanoball but does not indicate whether a LMCT or MLCT type interaction is occurring.

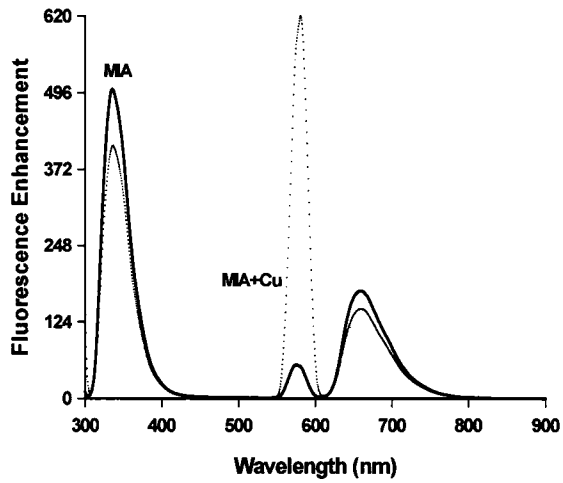

Figure 12 MIA and MIA+Cu in phosphate buffer

In an attempt to prove that this peak was due to LMCT, a colleague (and UPEI graduate) Wade White was contacted at Queens University. There they have the capability to perform HOMO-LUMO calculations on molecules in order to determine the type of

interaction which is occurring (LMCT, MLCT etc...). If the HOMO-LUMO gap is small it indicates a LMCT type of interaction whereas a large gap corresponds to MLCT. These calculations require the original x-ray crystal structure data and a very fast computer. Unfortunately after providing this information (x-ray crystal structure data obtained from the Zaworotko group) to this group at Queens, they were unable to perform these calculations on the nanoball because it is too large and complex a molecule for their method to handle. Usually this group deals with molecules of at most 30-40 atoms in size and since the time required for the calculation is based on the number of atoms squared, this in itself is a lengthy process. The nanoball however, is about twelve times larger than the molecules they are capable of dealing with. Therefore, the time constraints and computer software limitations combined just did not make doing this calculation feasible. So without computational evidence for the nanoball band at 448 nm, it is therefore a proposal, with some experimental support, that the band is due to a ligand-to-metal charge transfer (LMCT).

It was proposed that the third peak at 670 nm, which was weak, was just an integral wavelength multiple ghost of the first strong peak at 330 nm. To test this hypothesis three different cutoff filters were used to block out the light below 400 nm which would exclude the first peak at 330 nm. The three filters tried were: 1) a colorless filter (PIN 19FCG055), 2) yellow glass type filter (PIN 19FCT059) and 3) a yellow GG400 filter (PIN 19FCT057). The filters were placed in the emission slot of the fluorimeter separately and each filter scan showed the peak around 670 nm was eliminated. By using these filters to eliminate the strong band around 330 nm they also eliminated any weaker echoes of the peak at higher

wavelengths. Since the peak at 670 nm disappeared using the filters it proves that this 670 nm band is not a true peak as shown in Figure 13. It can also be seen in this Figure that the band at 448 nm is still present even when the filter was used which was expected since it is a true peak. After this discovery the subsequent MNB fluorescence scans were only done from 300-600 nm because that peak at 670 nm is no longer of any significance to observe in the scans.

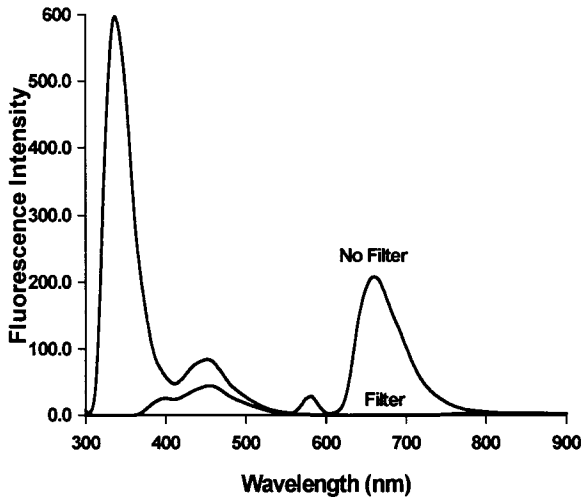

Figure 13 MNB and MNB with cutoff filter in phosphate buffer

III.3 *Host-Guest Fluorescence*

As shown previously the MNB absorbs from 250-400 nm so any guests chosen for inclusion with the nanoball need to absorb at a higher wavelength than 400 nm so there is no conflict between the spectra of the host and the guest. Potential guests must also fluoresce in a different region of the spectrum than the MNB or the two spectra will overlap

one another and make it difficult to determine if any effect is present. A large range of guests were tried in the host-guest experiments, these are summarized in Table 2.

Guests			
Pyridine	Biphenyl	Benzene	Pyrene
4,4'-Dipyridyl	p-Nitrophenol	Curcumin	Aniline
Hydroquinone	Benzoic Acid	2,6-ANS	Nile Red
Catechol	Resorcinol	2,6-TNS	Toluene
l-Tyrosine	Guanine	Phenol	1,8-ANS
o-Phenylenediamine	m-Phenylenediamine	Naphthalene	Xanthone
Anthracene	Nitrobenzene	Chlorobenzene	

Table 2 Guests used for host-guest experiments

As reported in the honours thesis the MNB formed a 1:1 complex with benzene.[20] Seeing how the previous work was done on the LS-100 fluorimeter another fluorescence titration with 0-40 mM benzene was done with the nanoball on the newer LS-55 fluorimeter used in this thesis work to make sure the same result was obtained and also to give an extra trial for a better average result, to lower the standard deviation of the binding constant K. As before this further trial confirmed that the second MNB peak at 448 nm did increase in intensity with increasing benzene concentration. Also the 1:1 fit gave a similar K value of 51.8 M^{-1} as compared to the previous average of 51.40 ±40 M^{-1} with a previous average reciprocal plot having an r value of the double reciprocal plot of 0.988. With all four trials

averaged the K value became 50±30 M^{-1} and the r value of the double reciprocal plot was improved to 0.996, which shows that the fourth trial was consistent and strengthened the existing result. This excellent linear correlation of the double reciprocal plot confirms that only 1:1 complexes are formed. Figure 14 shows (a) the fit of the fluorescence titration data according to Equation 5 and (b) the double reciprocal plot.

a) b)

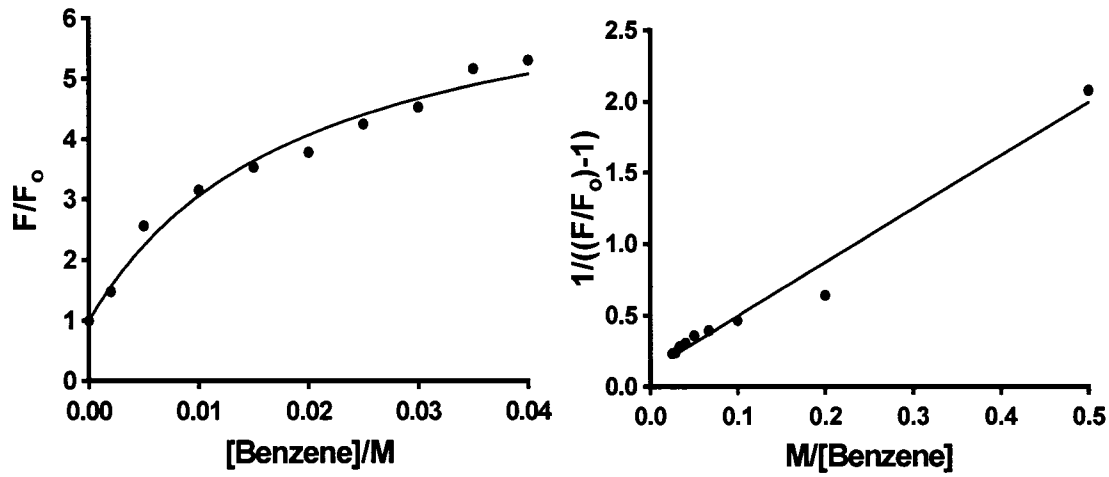

Figure 14 a) Average 1:1 fit and b) reciprocal plot for MNB+benzene

It is unexpected and surprising that the nanoball would only form a 1:1 complex with benzene, because it appears from all the potential binding sites that a small guest like benzene should be able to form a much higher order complex with the nanoball. Furthermore the complex would be expected to have a higher binding constant (K) because benzene is so small the nanoball should be able to bind the whole guest tightly. However, benzene may not be entering the methoxy nanoball interior cavity or shallow surface cavities

because the twelve solvent molecules (water) which can fit into the internal cavity may have more affinity for the nanoball than the benzene guest does. Therefore the water molecules could bind more strongly to the nanoball than the benzene and therefore prevent more than one guest from including and the weaker affinity for benzene results in the formation of a weakly bound (low K) complex with the nanoball. This provides another motivation for trying to discover another guest which will complex with the nanoball in this present work.

Other Attempted Guest Inclusions:

The following is a summary of other guests attempted for host inclusion into MNB, and the reasoning as to why they could not be used or why they were not studied further. These particular guests were chosen due to their aromatic nature and their size; because benzene worked it was predicted that other similar compounds would form complexes. These molecules also had polar group substituents which was thought might increase the solubility of the guests in the phosphate buffer, and enhance the binding. The solubility of these guests was tried at 40 mM because that was the maximum concentration used in the benzene trials.

Curcumin was chosen as a potential guest because it absorbs and fluoresces at higher wavelengths than the nanoball, so there would not be any interference. Also, since this molecule has two phenyl groups at either end separated by a large spacer backbone, it could potentially bind nanoballs together, *i.e.* it is the inclusion analog of a bidentate ligand in coordination polymer chemistry. Experiments were therefore conducted to see how the nanoball affected the solubility, absorbance and fluorescence of curcumin. However,

neither the absorbance or the fluorescence of curcumin changed upon addition of MNB and the solubility also remained the same. This may be due to steric interactions between the curcumin and the nanoball substituents or because of a size mismatch between the curcumin and the nanoball cavities not allowing the curcumin to enter and form a complex, especially as a result of the methoxy and hydroxy substituent in the benzene rings.

Toluene was found to be soluble in phosphate buffer at 40 mM. Therefore the fluorescence of the MNB was tested both alone and with toluene present to check for any effect which would indicate complexation. However, the fluorescence titration and the 1:1 fit showed no inclusion of toluene. This may possibly be due to steric interactions between the methoxy groups on the ligand (or the water and methanol templates) with the methyl groups on the toluene molecules. It is strange that benzene would include but just adding a methyl group to the guest (toluene) would result in no complexation. However, the benzene complex was only a weak 1:1 binding complex, probably due to steric interactions as mentioned previously. Therefore, it is possible that just that small addition of a methyl group increases the sterics and decreases the ability for the nanoball to bind the guest over the solvent enough to result in no complexation. It could also be a result of the electronic effects of the methyl group on the benzene π-system.

Both pyridine and biphenyl were soluble at 40 mM and were tried as potential guests. They each increased the MNB fluorescence intensity, but only very slightly. Separate fluorescence titrations were performed with both guests and MNB. After going from 0 mM to 40 mM of guest present the nanoball fluorescence changed very slightly. So when these results were fit to the 1:1 fit equation (Equation 5) the resulting fit was close to

a horizontal line as opposed to the desired curved fit. The observed flat line indicates little or no effect on the fluorescence and usually indicates scattered results. After 1:1 fit tests were determined to have no significant effect on the nanoball it was concluded that there was no complexation occurring, or if it was, the equilibrium constant K was too small to allow for its determination by this method ($K \leq 20\ M^{-1}$) .

The following guests were all soluble at 40 mM in the phosphate buffer, however they absorbed too strongly at 290 nm where the nanoball does, so they could not be used for host-guest studies: 2,6-ANS, 1,8-ANS, 2,6-TNS, 4,4'-dipyridyl, catechol, resorcinol, hydroquinone and benzoic acid. As for phenol the solubility and absorption were both acceptable but the molecule fluoresced too strongly where the nanoball did, so again there was conflict with the phenol fluorescence masking any potential effects of the nanoball fluorescence. So again this guest could not be used for fluorescence titration studies.

All of the molecules listed below could not be used for host-guest studies because they were not soluble in the phosphate buffer at 40 mM which was the maximum concentration used in the benzene host-guest studies. This concentration was used as a reference because if concentrations smaller than this were used the effect on the LMCT MNB peak fluorescence would not be as obvious for the fit studies because the peak intensity is so weak to begin with. The low solubility guests tried are as follows: naphthalene, anthracene, pyrene, nitrobenzene, aniline, chlorobenzene, m-phenylenediamine, p-nitrophenol, L-tyrosine, guanine and o-phenylenediamine.

Due to the solubility problems encountered with guests in the phosphate buffer it was decided to test the solubility of these same guests in water because it has a lower ionic

strength. It was previously noted in the honours work that MNB was water soluble and had a fluorescence spectrum in aqueous solution very similar to that in the phosphate buffer (330 and 447 nm as compared to 330 and 448 nm respectively). The following molecules were tested for their solubility at 40 mM in water: toluene, naphthalene, anthracene, pyrene, nitrobenzene, aniline and chlorobenzene. Only the aniline was soluble at 40 mM so the others were tried at 10 mM, and this time only toluene was water soluble.

A trial was run with MNB plus toluene in water by making up a 25 mL solution of MNB in water and then using 10 mL of this solution to make up a 10 mM toluene solution. A 10 mM toluene solution with no MNB was also made for comparison as well as just a water blank. The fluorescence spectrum of each of these solutions was then measured and then the areas of the spectra were compared. The water area was subtracted from the MNB in water area and the toluene in water area was subtracted from the MNB+toluene in water area so that the two MNB areas could be compared for any effect of toluene inclusion. However, it was discovered in the process that the toluene in water actually absorbed and fluoresced where the MNB does and therefore was not useful as a guest with MNB.

III.4 *pH Dependence*

As reported in the honours work[20], there was a pH dependence of the presence of the LMCT band in the MNB fluorescence spectrum. This band was observed in the phosphate buffer (pH=6.8), but it was weak in acetate buffer (pH=3.5). This suggests a significant pH dependence.

A further trial was carried out to try and achieve a better pattern and clearer picture

of this pH dependence. The fluorescence measurements for the low pH region ranged from pH 4.10-6.54, and the LMCT peak intensity increased from 9.2 to 30.4. For the higher pH measurements the solution contained pH ranges from 7.02-8.87 and the fluorescence intensity of the second peak ranged from 33.7-49.9. These two sets of data were combined in Figure 15 and a clearer reversibility was observed than that obtained previously. This result confirms the hypothesis established during honours work that this MNB system could be used as a reversible molecular pH sensor with further development, since the measured fluorescence intensity changes significantly, reproducibly and reversibly with pH.

a) b)

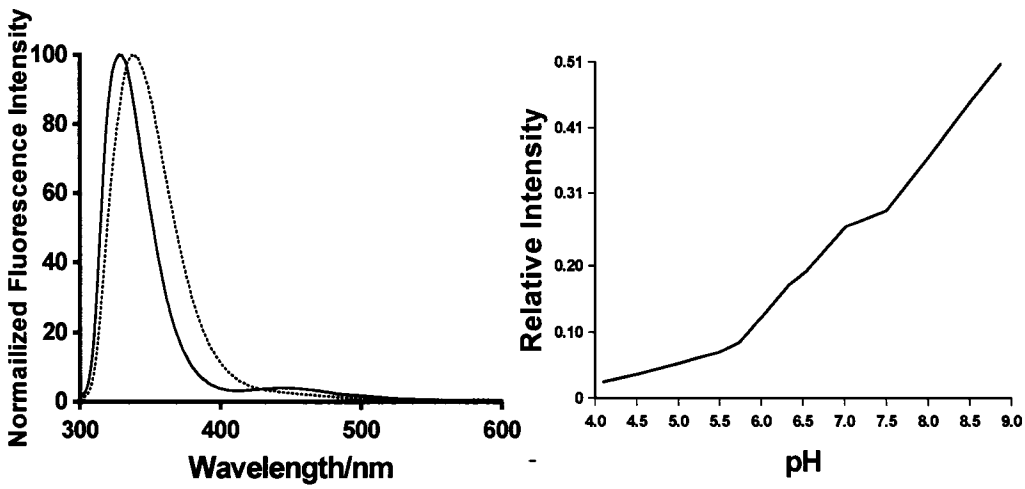

Figure 15 a) — MNB & ...MIA fluorescence spectra and b) intensity vs. pH

The LMCT band was not observed at low pH and the band intensity increased with increasing pH up to the maximum measured pH of 9. If the pH of a low pH solution was

increased then the LMCT band reappears; therefore the process is reversible. This pH reversibility could be due to quenching of this band by H^+, or by a reversible pH-dependent change in the structure of the nanoball or the nature of the excited state.

Just to ensure that the pH dependence was due to the nanoball and not the ligand a similar experiment was performed to increase the pH of a 5-methoxyisophthalic acid solution. The result confirmed what was already suspected, that the ligand shows no peak at higher pH however it does show a shoulder like peak at lower pH which is not present in the nanoball spectrum. Figure 16 compares the fluorescence spectra of the nanoball and the ligand at pH 5.49 and pH 5.47 respectively. This shows that the ligand displays a shoulder like peak at this lower pH when the nanoball does not show a peak. When the nanoball does show a peak at neutral pH the ligand does not, as seen previously. The fact that the ligand shows a peak at lower pH is not a concern because we are doing all of our host-guest experiments at neutral pH in the phosphate buffer when only the nanoball peak is present at 448 nm.

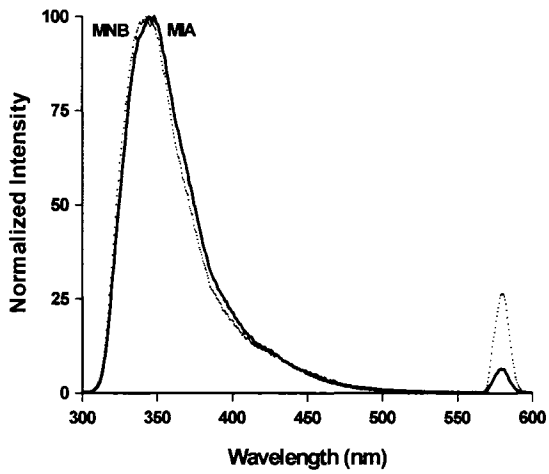

Figure 16 MNB & MIA fluorescence spectra at pH~5.5

III.5 *Thermodynamics*

After determining that a 1:1 complex existed between the MNB and benzene, and that no other guest was found which formed a complex with MNB, it was decided to study the thermodynamics of this host-guest complex. The fluorescence titration was completed as before but this time the temperature of the cuvette was controlled by using a water circulating bath. The first three trials were done at 8°C to check for any consistent pattern from which thermodynamic properties could be extracted. The average plot of the trials confirmed a good 1:1 fit complex (Equation 5) with an F/F_0 value of 6.03 and a K value of 22±10 M^{-1}. Thus, a significantly lower value of K was obtained at this lower temperature. The next temperature investigated was 32°C which confirmed a 1:1 complex but this time the K value also decreased, to 21±14 M^{-1}. By comparison, the studies done at room temperature (22°C) gave a 1:1 complex with a K value of 53±30 M^{-1}.

This does not give a linear pattern. It is more of a triangular trend which increases from 8°C to 22°C but then decreases from 22°C to 32°C. The usual situation involves a linear plot where K either increases with increasing temperature or decreases with increasing temperature. If the plot is linear this indicates that the enthalpy and entropy are constant over the temperature range used. In this case we have a non-linear plot which could indicate that the enthalpy and entropy are changing over this range in temperature. If there is a large change in the heat capacity upon complexation this could result in the temperature dependent enthalpy and entropy values. At this point the results indicate a curved van't Hoff plot with very small binding constants as shown in Figure 17. The relative error in each of the binding constants however, is so large that a horizontal line can be drawn

connecting the relative errors for each temperature. This result indicates that there may be no change in the K values at all with temperature. Therefore, conclusive thermodynamic results could not be obtained because the relative errors are too large. Further experiments were not performed, because of the low values of K involved. Past experiences indicated that the lowest value of K which can be measured in these fluorescence titration experiments is around 20 M^{-1}, close to the value obtained at 8 and 32°C.

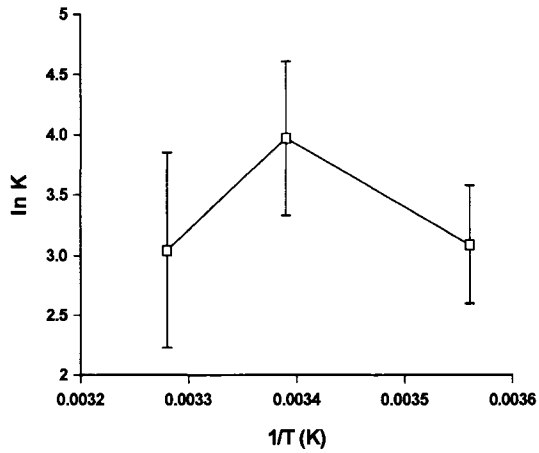

Figure 17 van't Hoff plot for MNB+benzene

III.6 *Time-Resolved Fluorescence*

The time-resolved fluorescence decays of the two nanoball peaks at 330 nm and 448 nm and comparison to the ligand peak decay were previously reported in my honours work.[20] The first MNB peak lifetime was 1.50 ns which compares very well to the lifetime of the ligand peak, 1.47 ns, confirming that this is a ligand-centred emission band. Both

of these peaks were fairly strong so that the decays were better and stronger than those of the second peak, when compared to the lamp profile. The second peak, assigned previously to an LMCT emission band, had a lifetime of 45 ns, but was very weak and scattered compared to the lamp profile. Therefore an effort was made to obtain a better decay curve for this peak in this present work. The time-resolved fluorimeter electrodes were adjusted and cleaned to get a maximum signal out of the excitation lamp to detect weak samples. It was also determined through trial experiments that the lamp profile was stronger at 300 nm than at the previously used 290 nm so this excitation wavelength should give a stronger signal.

This time the absorbance of the MNB solution used was not adjusted to between 0.25-0.35, but the solution was made as concentrated as possible to give the highest absorbance (1.09) and hence fluorescence intensity possible. The excitation wavelength was also increased to 300 nm to give stronger lifetime signal. Also, five individual sample scans were averaged to give a better signal-to-noise ratio. Although the steady-state fluorescence peak was still fairly weak, this procedure did give a stronger, smoother decay curve than before. The lifetimes for the first peak and the ligand were still similar (~1 ns) and the LMCT band of the MNB was still much larger (9.5 ns) so it confirmed previous results (See Figure 18).

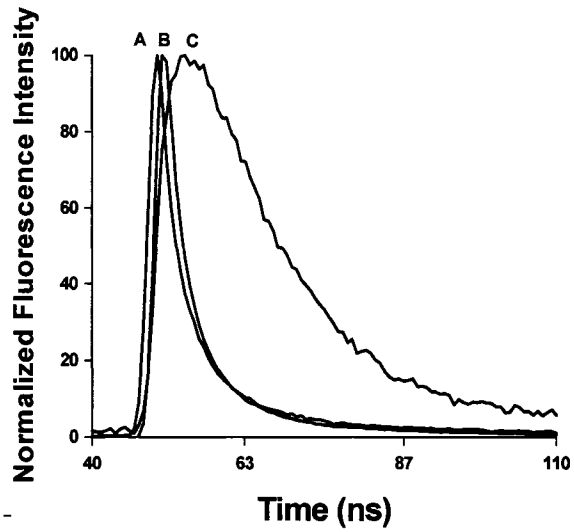

Figure 18 Time-resolved decay curves of **A** lamp profile, **B** MNB band 1 and **C** MNB band 2

To complement the steady-state host-guest experiments done with MNB and benzene, time-resolved experiments were also conducted under the same conditions. If only one type of complex is formed between benzene and methoxy nanoball molecules, the solution will have a double exponential decay, giving one value for the fluorescence lifetime of the complex and one for the free host. The ratio of the pre-exponential factors for these two lifetimes should change with increasing guest concentration. If upon complexation with MNB the benzene molecules experience several distinct environments, form several types of complexes with MNB, or they are even complexed to different degrees by the host, then multiple exponential decay constants (3 or more) will be obtained corresponding to a fluorescence lifetime for each of the different emitting species or environments. The 2.5mL saturated MNB sample was scanned with 0, 5, 10, 20, 30 and 40 mM benzene additions and

the lifetimes compared. There was no pattern occurring in the recorded lifetimes with increasing additions of benzene, as can be seen in Table 3, so this experiment did not provide any useful results. This was probably due to the weak nature of this LMCT peak being too small in intensity to yield accurate results. However, all decays gave very good single exponential fits, (excellent χ^2 values near 1.00) indicating that a single type of complex is formed, with no range in benzene-nanoball interaction. Therefore there was no significant effect of benzene complexation on the MNB lifetime.

[Benzene] (mM)	Lifetime (ns)	chisq
0	6.97	1.51
5	7.56	1.05
10	8.41	1.21
20	6.76	1.03
30	6.56	1.11
40	7.70	0.995

Table 3 Lifetimes of MNB with benzene additions

The MNB-pyrene system described in the following section on encapsulated guests was also investigated using time-resolved fluorescence. This was done to determine if there was any change in the lifetime of the combined system compared to just the nanoball itself to indicate some effect due to the presence of the pyrene. However, the lifetime of the purged MNB-pyrene system (0.90 ns) was much the same as the lifetime of the purged MNB alone (0.78 ns). So the pyrene also has little effect on the overall structure with the

MNB as was seen in the steady-state results described in the next section.

III.7 *Synthesis of MNB with Encapsulated Guests*

Since the goal of this project was to find some guests that would form complexes with this and other fluorescent hosts it was decided to try and incorporate such guests in the actual structure of the nanoball during its synthesis, as opposed to forming inclusion complexes in solution, which had proved fruitless, other than with benzene. The following three guests were attempted to be incorporated into the MNB structure: naphthalene, pyrene and Nile Red.

Although the naphthalene-nanoball system was darker green in color and did form crystals it is believed that it did not give the desired encapsulation. The absorbance should have differed from that of the nanoball itself. However, the absorption spectrum of the napthalene-nanoball system was only slightly broader but identical in shape to the nanoball spectrum, with no characteristic naphthalene peaks. The fluorescence of the complex was also identical to that of the nanoball. A solution of just naphthalene was made for comparison and it was found to absorb and fluoresce in the same region as the complex so it was masking the effect of the complex. Therefore, one cannot tell whether both naphthalene and the nanoball are present in the crystal or not, although the color change suggests this. These two factors lead to this attempt being put to rest. Single crystal x-ray diffraction may be attempted in the future, to determine the structure.

The pyrene-nanoball system also formed crystals which were a brighter green this time. The absorption spectrum of this system was also identical to that of the nanoball, only

slightly broader. Although small shifts were observed in the pyrene-nanoball spectrum, direct evidence of the presence of guest were not indicated in the spectrum. However, the fluorescence of the pyrene-nanoball solution was the same as the nanoball spectrum, except it contained more peaks which were indicative of pyrene present in the compound, shown in Figure 19 . When the complex was excited at the nanoball excitation wavelength, 290 nm, the spectrum looked like that of the nanoball and when it was excited at pyrene's excitation wavelength, 330 nm, the spectrum looked like that of pyrene, indicating that both species are present in the crystal.

If the pyrene was actually encapsulated in the nanoball structure it is expected that the new system should have its own unique fluorescence signal which differs from that of both the nanoball and pyrene separately. It has been published previously that the first (I_1) and third (I_{111}) vibronic bands of pyrene shift intensity upon changing the polarity of its environment.[55] Therefore, the band intensities should change upon going from a polar medium, phosphate buffer, to a non-polar medium, MNB cavity, if encapsulation is occurring. Upon comparison, the I_{111}/I_1 ratio for pyrene in the buffer was 0.37 and the pyrene-MNB system was 0.46. Although this is a small difference, it is significant, and provides evidence that the pyrene is indeed encapsulated inside the interior of MNB. Again, x-ray diffraction may be pursued in the future to determine this structure and prove conclusively inclusion.

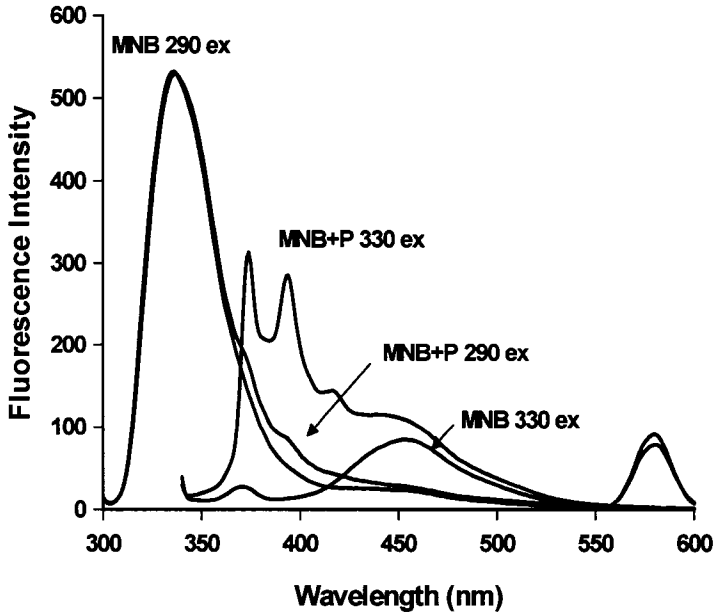

Figure 19 Fluorescence spectra of MNB synthesis with pyrene

Adding Nile Red resulted in the formation of purple crystals. The resulting absorption spectrum showed absolutely no change from the MNB spectrum. The nanoball and the Nile Red-nanoball solutions were excited at both 290 nm and 540 nm, to check both host and guest fluorescence respectively. At the nanoball wavelength, 290 nm, the spectrum was identical to the nanoball but at the Nile Red wavelength, 540 nm, no fluorescence was observed. This is not surprising, because Nile Red is much larger than the other two guests investigated and is probably too large to fit into the MNB cavity. Therefore, this approach

was abandoned because the Nile Red was clearly not included in the nanoball structure and had no effect on its spectrum.

III.8 *MNB as a Guest*

After examining and exhausting all possibilities for guests to be included in the MNB it was decided to try including MNB as a guest into larger hosts, namely cyclodextrins. Four different cyclodextrins were investigated for this process: β-CD, HP-β-CD, γ-CD and HP-γ-CD. It was discovered that in fact the using 290 nm excitation, the cyclodextrins themselves fluoresced very slightly in the same area as the nanoball LMCT band which is very weak in nature so even the small fluorescence signal from the cyclodextrins competes with the LMCT band. Therefore when subtracting the effect of the isolated cyclodextrins from the CD-MNB complex fluorescence scan, there was no effect on the fluorescence scan when compared to the isolated MNB spectrum. So it was proposed that in each of these cases the cyclodextrins have little interaction with the MNB to form complexes, rather the fluorescence spectra were just due to combinations of the fluorescence signals of the individual components.

III.9 *MNB Conclusions*

The biggest issue with the MNB was finding guests that were soluble in the phosphate buffer which gave the strongest MNB fluorescence signal, especially for the LMCT band which was of greatest interest particularly for host-guest studies. Also the fact that the MNB absorbed at such a low wavelength in the electromagnetic spectrum (~290

nm) created a problem. This is because most molecules and all the common guests tried also absorb in this area so there was a conflict with the guests interfering with the MNB absorption. Therefore information on potential complexes formed could not be obtained from a spectrum because of all the unwanted signals centered in that area. The same situation occurs with the potential guests fluorescing in the same area as the host, which also causes conflict between the fluorescence signals.

Another issue is cavity size, intermolecular binding strength and sterics from the methoxy substituents and the water and methanol templates present in the nanoball structure. Benzene was the only guest for which inclusion occurred, this was probably due to cavity size and benzene being small and not having any substituents for steric hinderance to occur. But even so the average binding constant only turned out to be $50\pm30\ M^{-1}$ which is extremely weak. Therefore the electronic nature of the nanoball-guest interaction must be so weak that it does not allow for strong intermolecular binding to form complexes. The MNB may have a better interaction with larger guest molecules if the binding is based on polarity or hydrogen bonding etc. which benzene is not capable of doing, it may also be able to bind anions. This would explain why none of the other potential guests tried formed complexes with the MNB. Also this simple 1:1 inclusion complex with benzene is surprising given the large number of cavities on the nanoball surface.

It was attempted to get crystal structures of the MNB synthesized in our lab from the Zaworotko group at the University of South Florida. However, they were not stable enough to survive the jostling of the transport and degraded on the way. It would have been interesting if ever it were possible to have a crystal structure done on site to get a structure

of the MNB itself and also the MNB-benzene complex (if it could be crystallized) to get a definitive answer as to what type of binding and interactions are actually occurring within the nanoball-benzene complex. This may help determine if there is anything that can be done to achieve the inclusion of other guests. As of now these results discourage the idea that the nanoballs can be used as nodes or ball bearings in the construction of nanomachines because of the weak binding and lack of inclusion.

In conclusion, the MNB exhibits LC fluorescence and a LMCT fluorescence band, which is sensitive to complexation with benzene. The MNB CT fluorescence is reversibly pH-sensitive. Also the nanoball forms a 1:1 complex with benzene with a relatively weak binding constant of $50\pm30 M^{-1}$. So far there has been no success in finding another guest for complexation. Since no larger guests have been included it is unlikely that nanomachines could be made with this nanoball by inclusion of one guest into two nanoball hosts by forming a 2:1 complex. However, the results for encapsulation of guests during the MNB synthesis are very promising. This may represent a useful application of MNB as a fluorescent host.

IV. *Results and Discussion: Cucurbit[6]uril Analogue*

The LB[6] used for this project was received from Lyle Isaacs' group at the University of Maryland, who collaborated on this work. Isaacs' group in collaboration with our group had previously studied a wide range of guest molecules including alkanediamines, aromatics, aminoacids and nucleobases with LB[6] to determine the effects of the size, shape and substituents on the binding properties of LB[6].[46,56] Therefore, the goal of this project was not to examine a wide range of guests to determine the fluorescence binding abilities. However, it was desired to examine a few systems including bidentate guests to determine their potential for forming higher order complexes with LB[6] which may possibly form the basis for nanostructures. It was also desired to establish time-resolved and thermodynamic data for LB[6] and its complexes.

Jason Lagona (for whom the compound was named) synthesized this host for us, but finished his PhD during the time frame of this project. Therefore, he was no longer able to synthesize and supply us with the LB[6] we needed for further experiments, so we worked with the existing supply. Only a limited supply of LB[6] (25 mg) was available for experimentation. Also, as previously mentioned, the synthesis was deemed too difficult and dangerous for us to recreate in our physical chemistry laboratory. Therefore, efforts were made to conserve this supply while conducting as many experiments as possible. The fluorescence of 12.5 μM LB[6] was found to be stable over a period of 2.5 hours, so this does not present a problem over the course of time required for a fluorescence titration to be carried out.

IV.1 *UV-Vis Absorption*

The absorption spectrum of LB[6] was acquired in acetate buffer. This spectrum, as seen in Figure 20, shows a strong absorbance from 250nm to 425 nm. Absorption in this range presents the same problem seen with the methoxy nanoball. Guests chosen for inclusion must not absorb in this area, which leaves a very limited number of guests for which studies can be performed.

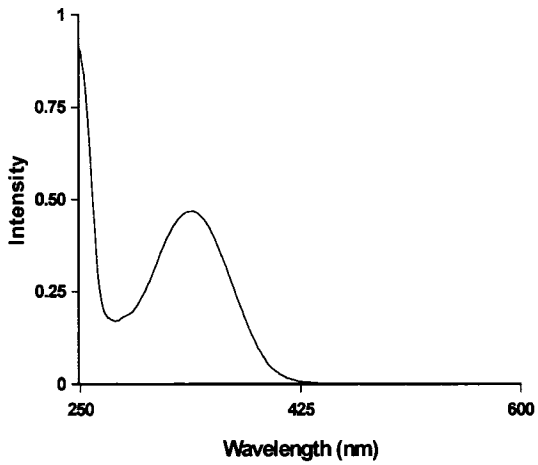

Figure 20 Absorption Spectrum of LB[6] in acetate buffer

IV.2 *Steady-State Fluorescence Spectra*

The steady-state fluorescence spectrum of LB[6] was acquired using λ_{ex}=337 nm and can be seen in Figure 21. This spectrum shows a strong peak around 510 nm and a weak

solvent Raman peak at 400 nm. The peak of interest to perform fluorescence studies on is the peak at 510 nm.

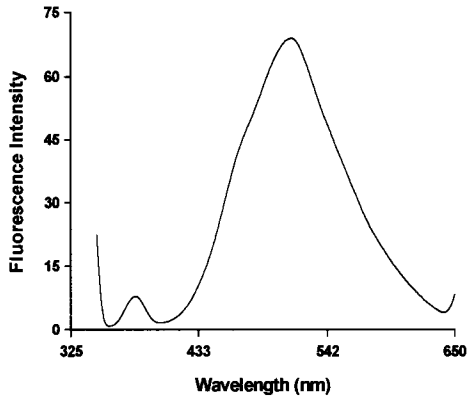

Figure 21 Fluorescence Spectrum of LB[6] in acetate buffer

IV.3 *Host-Guest Fluorescence*

The first guest attempted was curcumin, as this guest had been studied before in our group with modified cyclodextrins[57] and CB[6][58] and is expected to be a good size match for LB[6]. Furthermore, it contains two symmetrical ends, which makes it likely to form 2:1 host-guest complexes, as observed with both cyclodextrins and CB[6]. Since both the host and the guest in this situation are fluorescent the fluorescence titrations were tried both ways; *i.e.* first by studying the effect of LB[6] on the fluorescence of curcumin, and then the effect of curcumin on the fluorescence of LB[6].

For the first situation where the effect of LB[6] on curcumin was studied six trials were performed and are outlined below:

For Trial 1 there was no pattern to the resulting effect on the fluorescence spectrum, and the results did not fit well to either a 1:1 or a 1:2 host-guest complexation product. These are the only two complexes for which a fit program is currently available. It was thought that because such a small amount of LB[6] was used (0.0002 g) to make this solution it was too imprecise for measurement, so another trial was performed.

In the second trial, a larger amount of LB[6] was used but again the results were scattered. The resulting fit data did not correspond well to either a 1:1 or a 1:2 complex. Since the double reciprocal plot was definitely non-linear it was clear that the complex was not 1:1. However, the 1:2 fit obtained was also not great, so it was not clear what type of complex was being formed .

Another trial was done to try and improve the data and see if there was any effect of the LB[6] on its own that was interfering with the fluorescence data. This trial showed that there was no effect of the LB[6] itself on the fluorescence in this area so that eliminated a possible complication with this system and this set of titrations was not repeated in further trials. However, the fit again did not correspond well to either a 1:1 or a 1:2 complex. It was agreed that it was not a 1:1 complex due to the non-linear reciprocal plot and since the 1:2 fit was not good either it was proposed that there were not enough points in the current titrations to allow the fitting program to fit the data properly.

Trial four made dilutions of a quarter each time from 25 μM to 0.33 μM. This method showed a clear decrease in the fluorescence intensity of the peak with increasing LB[6] concentration, which is known as fluorescence suppression. However, yet again the data did not fit the 1:1 or the 1:2 equations very well. Therefore two further trials were done

under these same conditions with these same dilutions for comparison. Again in both cases the fluorescence intensity of the peak decreased with increasing LB[6] concentration but the data did not correspond to either a 1:1 or a 1:2 complex (See Figure 22 and Figure 23).

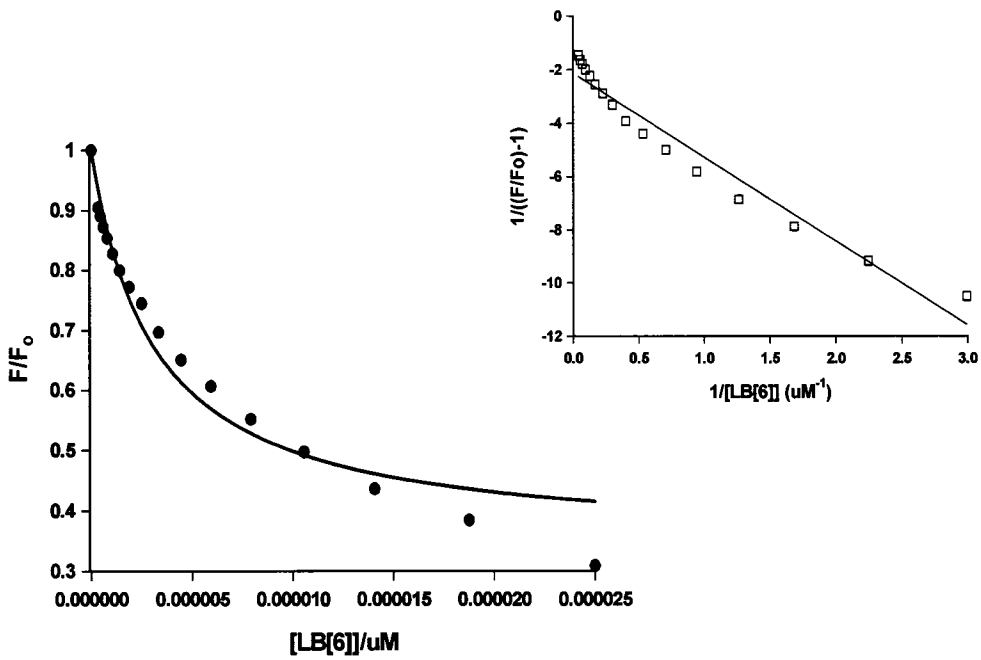

Figure 22 Average 1:1 fit and reciprocal plot (inset) for Curcumin+LB[6] fluorescence

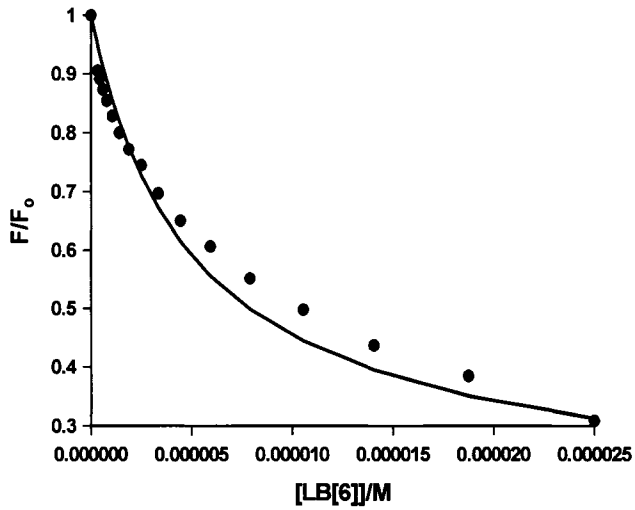

Figure 23 Average 1:2 fit for Curcumin+LB[6] fluorescence

At this point it was thought that there may be a higher order complex being formed between the LB[6] and the curcumin. However, only1:1 and 1:2 fit programs are available at this time. So the development of a fit equation for 2:1 and 2:2 complexation models was attempted. The following equations were derived for a 2:1 (Equation 17) and 2:2 (Equation 18) host:guest complexation model using the same methods used for the development of the existing 1:1 and 1:2 equations.[59-61]

$$F/F_o = \frac{1+F_1K_1[H]_o+F_2K_1K_2[G][H]_o}{1+K_1[H]_o+2K_1K_2[G][H]_o} \qquad (17)$$

$$F/F_o = \frac{1+F_1K_1[H]_o+F_2K_1^2K_2[G][H]_o^2}{1+K_1[H]_o+2K_1^2K_2[G][H]_o^2} \qquad (18)$$

In both Equations 17 and 18 the [H] and [G] would be switched for the case of host fluorescence.

The derivation of the 1:2 equation for guest fluorescence was based on the step-wise derivation of the known 1:1 fit equation (Equation 5); this will correspond to a 2:1 equation for host fluorescence where the guest (G) is non-fluorescent, and is outlined below:

First we establish the equilibrium for 1:1 complex formation (K_1) where G is the guest and H is the host.

$$G + H \rightleftarrows (G:H) \qquad K_1 = \frac{[(G:H)]}{[G]\,[H]} \qquad ①$$

Then the equilibrium for an additional guest (G) adding to the existing 1:1 complex is set up.

$$(G:H) + G \rightleftarrows (G_2:H) \qquad K_2 = \frac{[(G_2:H)]}{[(G:H)][G]} \qquad ②$$

If we assume $[H]_o >> [G]_o$ (can set up the experiment this way),

then $[H] = [H]_o$ ③

So therefore by making substitutions of ③ into ①

$$K_1 = \frac{[(G:H)]}{[G]\,[H]_o}$$

After rearranging equations ① and ② we get useful equations from K_1 and K_2:

$$[(G:H)] = K_1\,[G]\,[H]_o \qquad ④$$

$$[(G_2:H)] = K_2\,[(G:H)]\,[G] \qquad ⑤$$

Then substituting ④ into ⑤ this we get ⑥:

$$[(G_2{:}H)] = K_2 K_1 [G]^2 [H]_o \qquad ⑥$$

A few assumptions must be made at this point:

1) Assume H is non-fluorescent for derivation with non-fluorescent host; Assume G is non-fluorescent for derivation with non-fluorescent guest

2) Let F = integrated fluorescence emission

3) Have 3 emitting species G, (G:H), $(G_2:H)$

4) Each has extinction coefficient ϵ, ϵ', ϵ'' and rate constants for fluorescence k_F, k_F', k_F'' respectively.

Therefore in the presence of H:

$$F = \epsilon k_F [G] + \epsilon' k_F'[(G:H)] + \epsilon'' k_F''[(G_2:H)] \quad ⑦$$

and in the absence of H:

$$F_o = \epsilon k_F[G]_o \qquad ⑧$$

Define F/F_o as the enhancement caused by H:

$$F/F_o = \frac{\epsilon k_F[G] + \epsilon' k_F'[(G:H)] + \epsilon'' k_F''[(G_2:H)]}{\epsilon k_F[G]_o}$$

$$F/F_o = \frac{[G] + F_1[(G:H)] + F_2[(G_2:H)]}{[G]_o} \qquad ⑨$$

Where $F_1 = \frac{\epsilon' k_F'}{\epsilon k_F}$ = enhancement if all G is in 1:1 complex

$F_2 = \frac{\epsilon'' k_F''}{\epsilon k_F}$ = enhancement if all G is in 1:2 complex

Now we have more relationships:

$$[G]_o = [G] + [(G:H)] + 2[(G_2:H)] \qquad ⑩$$

So after substitution into ⑨:

$$F/F_o = \frac{[G] + F_1[(G:H)] + F_2[(G_2:H)]}{[G] + [(G:H)] + 2[(G_2:H)]} \qquad ①①$$

We want an equation in terms of $[H]_o$, K_1, K_2, F_1 and F_2 only ($[H]_o$ will be the independent parameter, K_1, K_2, F_1 and F_2 will be the fit parameters)

We can write equation ①① as the sum of three terms:

$$F/F_o = \underbrace{\frac{[G]}{[G] + [(G:H)] + 2[(G_2:H)]}}_{❶} + \underbrace{\frac{F_1[(G:H)]}{[G] + [(G:H)] + 2[(G_2:H)]}}_{❷} + \underbrace{\frac{F_2[(G_2:H)]}{[G] + [(G:H)] + 2[(G_2:H)]}}_{❸} \qquad ①②$$

$$❶ = \frac{1}{1 + \frac{[(G:H)]}{[G]} + \frac{2[(G_2:H)]}{[G]}}$$

$$\frac{[(G:H)]}{[G]} = K_1[H]_o \qquad \text{(from ④)}$$

$$\frac{[(G_2:H)]}{[G]} = K_2K_1[G][H]_o \qquad \text{(from ⑥)}$$

$$\therefore ❶ = \frac{1}{1 + K_1[H]_o + 2K_2K_1[G][H]_o} \qquad ①③$$

$$❷ = \frac{F_1}{\frac{[G]}{[(G:H)]} + 1 + \frac{2[(G_2:H)]}{[(G:H)]}}$$

$$\frac{[G]}{[(G:H)]} = \frac{1}{K_1[H]_o} \qquad \text{(from ④)}$$

$$\frac{[(G_2:H)]}{[(G:H)]} = K_2[G] \qquad \text{(from ⑤)}$$

$$❷ = \frac{F_1}{\frac{1}{K_1[H]_o} + 1 + K_2[G]} \quad ①④ \quad \text{X} \quad \frac{K_1[H]_o}{K_1[H]_o} = \frac{F_1K_1[H]_o}{1 + K_1[H]_o + 2K_2K_1[G][H]_o}$$

$$❸ = \frac{F_2}{\frac{[G]}{[(G_2:H)]} + \frac{[(G:H)]}{[(G_2:H)]} + 2}$$

$$\frac{[G]}{[(G_2:H)]} = \frac{1}{K_2[(G:H)]} \qquad \text{(from ⑤)}$$

$$\frac{[(G:H)]}{[(G_2:H)]} = \frac{1}{K_2[G]} \qquad \text{(from ⑤)}$$

$$❸ = \frac{F_2}{\frac{1}{K_2[(G:H)]} + \frac{1}{K_2[G]} + 2} \quad X \quad \frac{K_2[(G:H)]}{K_2[(G:H)]} = \frac{F_2 K_2[(G:H)]}{1 + K_1[H]_o + 2 K_2K_1[G][H]_o}$$

$$❸ = \frac{F_2K_2K_1[G][H]_o}{1 + K_1[H]_o + 2 K_2K_1[G][H]_o} \qquad \frac{[(G:H)]}{[G]} = K_1[H]_o \quad [(G:H)] = K_1[G][H]_o$$

Combining equations ❶,❷and ❸ gives:

$$F/F_o = \frac{1 + F_1K_1[H]_o + F_2K_2K_1[G][H]_o}{1 + K_1[H]_o + 2 K_2K_1[G][H]_o} \qquad (17)$$

The equation for the 2:2 complex was derived in the same way. The only difference was that the K_2 equation was set up as:

$$(G:H) + (G:H) \rightleftharpoons (G:H)_2 \qquad K_2 = \frac{[(G:H)_2]}{[(G:H)]^2} \; ①⑤$$

However, the problem with Equations (17) and (18) is that they still contain the variable of free host concentration [H] which is unknown. An extensive attempt was made to rearrange these equations and make substitutions in order to eliminate this variable. Unfortunately this resulted in equations which were even more complicated and still contained unknown host variables. Therefore these equations in their current form are of no real use. So until some useable equations are developed for a fitting program this complex formation between LB[6] and curcumin will just be assumed to be some type of higher order complex.

The following tables (4&5) summarize the results of both the 1:2 and 1:1 fit results for curcumin guest fluorescence as a function of LB[6] host concentration.

Trial	F_a	K_1 (M^{-1})	F_b	K_2 (M^{-1})	chisq
4	0.28	$1.5x10^4$	0.27	$4.7x10^6$	0.00
5	0.06	$3.6x10^4$	0.39	$7.6x10^6$	0.02
6	0.01	$1.8x10^4$	0.45	$1.1x10^6$	0.01
Average	0.20	$2.0x10^5$	0.03	$1.0x10^3$	0.01

Table 4 Summary of 1:2 Curcumin+LB[6] results

Trial	AA	K (M^{-1})	chisq
4	-0.94	$1.7x10^5$	0.00
5	-0.75	$3.7x10^5$	0.01
6	-0.74	$1.0x10^5$	0.00
Average	-0.66	$3.2x10^5$	0.01

Table 5 Summary of 1:1 Curcumin+LB[6] results

The inability to fit this data to either a 1:1 or a 1:2 complex supports the idea that a higher order complex is being formed which is desired. There may in fact be chains forming with the curcumin molecules joining the LB[6] host molecules together. In the future crystallization should be attempted to determine the structure, stoichiometry and the actual type of complex that is formed.

The other way to look at complex formation between these two molecules is to consider the effect of curcumin on LB[6] fluorescence. However, the curcumin solutions made up in the acetate buffer were concentrated due to solubility issues, so the exact concentration was not known. Three trials were done anyway by starting with the

concentrated solution and dilutions to see the effect on the LB[6] fluorescence. The results from these trials were different from one another and the data points were scattered. It was proposed that this was due to the low concentration of the curcumin in solution so the concentration of the solution was determined. This was done by preparing a $2.5x10^{-4}$ M curcumin in 50 mL of methanol in which curcumin is soluble. After the solution sat overnight 12 μL of this solution was added to 25 mL of acetate buffer to make a $2.0\ x10^{-8}$ M solution of curcumin in acetate buffer. Then a concentrated curcumin solution was made in acetate buffer for comparison and it too was left overnight and then filtered. Then the absorbance of both solutions were taken and compared using 1 cm^2 quartz cuvettes. The $2.0\ x10^{-8}$ M solution absorption was 0.10 at 260 nm, while the concentrated solution absorption was 0.04 at 260 nm. So using Beer's Law ($A=\epsilon cl$) and the known concentration (c) $2.0\ x10^{-8}$ M, absorbance (A) 0.10 and pathlength (l) of 1 cm the molar absorptivity ϵ was determined to be $4.8x10^{6}\ M^{-1}cm^{-1}$. Then ϵ was used with the concentrated solutions absorption to determine the concentration of the saturated solution. The concentration was determined to be $9.0\ x10^{-9}$M which is very low.

Therefore these trials most likely did not work because the concentrated curcumin solution being used had a concentration of $9.0\ x10^{-9}$M to start with which was followed by subsequent dilutions. Experiments are usually performed with enough guest present to acquire a fluorescence spectrum. In this case the $9.0\ x10^{-9}$M solution was a result of a concentrated curcumin solution so this was the maximum amount of curcumin that could be present in the solution. However, this concentration did not give a good fluorescence signal and the solution was then diluted for the other concentrations so the fluorescence was

even weaker. Therefore the solution of guest was too weak to get a fluorescence signal so these results were not useful.

Knowing that aromatic molecules formed inclusion complexes with LB[6], other guests of similar structure were tried and are summarized in Table 6.

Guests			
Benzene	Phenol	Nile Red	Xanthone
Curcumin	Naphthalene	Toluene	Anthracene
2,6-ANS	Pyrene	1,8-ANS	Nitrobenzene
2,6-TNS	Aniline	Phenylenediamine	Chlorobenzene

Table 6 Guests used in host-guest experiments

Each of the following molecules were used to make 25 μM solutions in acetate buffer to test their solubility: toluene, phenol, chlorobenzene, 2,6-ANS, 1,8-ANS, 2,6-TNS, naphthalene, xanthone, anthracene, pyrene, nitrobenzene and aniline. The 25 μM concentration was chosen as a reference because this was in the range of concentrations used for the benzene experiments with MNB. Of all these guests only 1,8-ANS and toluene were soluble at 25 μM in the acetate buffer.

A fluorescence titration was attempted with 1,8-ANS to see the effect LB[6] had on its fluorescence. However, the LB[6] and the 1,8-ANS both absorb and fluoresce in the same region as one another and therefore compete with one another's signal. A guest is required which absorbs at a wavelength higher than 400 nm. Unfortunately toluene also

absorbed and fluoresced in the same region as LB[6] and could not be used for host-guest studies.

IV.4 *Thermodynamics*

After our previous determination that a 1:1 complex was formed between LB[6] and benzene[46] it was decided to study the thermodynamics of this system in this project. The fluorescence titrations were performed as before for the host-guest studies, but this time the temperature of the cuvette was controlled using a water circulating bath. One trial was performed at 8, 15 and 32°C due to the limited supply available and the three trials at 22°C were used from previous work.[46] The average K value at 22°C was determined to be 6900 M^{-1}, this was used as a reference point for the other temperatures. At 8°C the fluorescence titration resulted in a 1:1 fit giving a K value of $1.56x10^4 M^{-1}$. Therefore, it was thought at this time that the binding constant, K, was decreasing with increasing temperature.

The next temperature studied was 32°C to see if the trend continued. At 32°C the resulting K value was determined to be $8.81x10^3$ M^{-1}. This did not fit the suggested trend, so with the remaining supply of LB[6] it was decided to try 15°C to check for a trend in K value. Unfortunately the binding constant at 15°C was $1.57x10^4$ M^{-1} which is even greater than the K value at 8°C. Therefore, there does not appear to be any trend in the binding constant value with temperature. This result may be because the fluorescence peak being studied is not very strong. The van't Hoff plot in this case could be curved, as seen with the MNB, indicating that ΔH and ΔS are not constant over the given temperature range. Further trials would need to be performed to establish a trend, and standard deviations, if more

LB[6] sample can be obtained in the future.

IV.5 *Time-Resolved Fluorescence*

As determined in previous work[46] LB[6] forms a 1:1 complex with benzene. The time-resolved fluorescence decays of both LB[6] and LB[6] plus 10 mM benzene were performed for comparison. For the LB[6] itself, the lifetime was fairly small, 0.420 ns, which confirms our previous results.[46] This was expected because the quantum yield for LB[6] is low, 0.0023,[46] indicating the fluorescence is relatively weak and short-lived. Including the 10 mM benzene increased the lifetime only slightly to 0.633 ns. The small increase in lifetime agrees with the steady-state results which gives only a small increase in F/F_0 value for inclusion of 10 mM benzene from 1 to 2.40. Figure 24 shows the time-resolved spectra for the lamp profile, LB[6] and LB[6] + 10 mM benzene. Since the lifetime of the complex as well as the free host is so short, it is not possible to use lifetime measurements to study the complexation process.

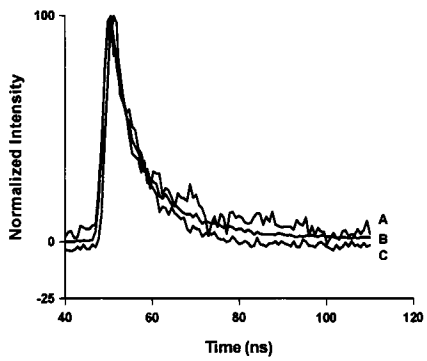

Figure 24 Time-resolved decay curves of **A** LB[6], **B** lamp profile and **C** LB[6]+10 mM benzene

IV.6 *Cucurbit[6]uril Analogue Conclusions*

LB[6] has huge potential as a fluorescent host due to the size and shape of the cavity; it can accommodate many larger guests than the original CB[6]. A wide range of guests were studied with this host in previous and concurrent work with our collaborator Lyle Isaacs at the University of Maryland during the course of this project, in which the binding properties of LB[6] with guests with various substituent groups like amines were examined. Therefore, it was desired to focus on examining more of the properties of LB[6] like lifetime and thermodynamics for a specific host-guest system including bidentate guests rather than investigating many guests for host-guest properties.

The problem with LB[6] again is the solubility issue of most common guest molecules in the acetate buffer. Harsher solvents that may dissolve the guests better will degrade the host so host-guest studies cannot be done. Also the LB[6] absorbs and fluoresces at such low wavelengths that guests have to be found that absorb and fluoresce in different areas at higher wavelengths than the host to avoid conflict.

The lifetime of the LB[6] was found to be quite small due to the relatively weak fluorescence of this compound, which results in it being short-lived. Curcumin was the only guest for which host-guest inclusion results could be obtained due to the solubility and absorbance issues previously mentioned. Even with this host-guest system it was unclear what type of complex was being formed, due to the lack of higher order fit equations currently available. It may be possible that a fit could not be obtained because LB[6] was forming long chain complexes with curcumin as a joiner. This type of higher order complex would explain the lack of 1:1 or 1:2 fits which are available. Also, the thermodynamic data

established for LB[6] and benzene were very scattered. This is very encouraging and promising, in terms of the described goal of forming large, fluorescent nanostructures through supramolecular chemistry. However, there is simply no more LB[6] available. If more LB[6] could be obtained it may be possible in the future to perform further experiments to establish conclusive trends and data.

V. *Results and Discussion: Bistren Cage*

The bistren cage was explored because like the previous two hosts, this cage also displays fluorescent properties. All of the initial work done with the bistren cage is described in a *Chemical Communication* paper by the group of Fabbrizzi in 1998.[7] This article outlined the synthetic procedure, but after further investigation it was realized that it described little else in terms of characterization or fluorescent properties. This group presented a lot of results without key details for their reproduction by other groups. We attempted to contact Fabbrizzi on several occasions without response. After extensive searching it was found that no other fluorescence work had been done with this particular bistren cage other than that presented by Fabbrizzi in this one article. It was also discovered that Fabbrizzi had no European or North American patents on this cage or this work so it was strange that we received no communication from him on the subject at all. It was especially strange since he had given permission to Dr. Wagner previously to include this paper in a book chapter on fluorescent hosts. Therefore it became necessary to find our own techniques for characterization and verification that the desired cage was synthesized before further fluorescence experimentation was done. This also meant, however, that the host properties of this interesting cage compound were previously unexplored, offering the opportunity for a wide range of experiments to be conducted.

V.1 Synthetic Difficulties

The synthetic procedure (as outlined in chapter II.2.3) was attempted several times. The first attempt seemed to be going well after the first step which yielded an orange oil as expected and when the NMR was compared with that published in the article (for this intermediate compound)[50] it was very similar. Therefore it was encouraging that the correct product was made to this point. However, the following steps yielded a very viscous brown liquid instead of the indicated yellow-gold solid of the final product. After examining the NMR data of the product it was unclear whether the correct product was made because of the weak peaks and the extra peaks which were probably impurities. Also a ^{13}C NMR could not be obtained so this was not available for comparison.

Initially it was thought that placing the oil under high vacuum for 2 hours would draw the excess liquid off leaving a solid. However, this just resulted in bubbles forming in the oil resembling a marshmallow. It was pointed out that these amine cage systems are protonated in acid solution and will yield a solid more easily. Therefore, the oil was dissolved in 5 mL of 1M HCl. After dissolving in acid the solution was rotovapped to see if a solid would result. Although it was less oily than the original the product was still a bit wet and brownish in color. Samples were prepared for NMR regardless, again the spectra showed impurities and were not very diagnostic.

At this stage the ^{1}H NMR of the 9,10-bis(chloromethyl)anthracene (9,10-BCA) starting material was done in $CDCl_3$ for comparison to the product and to the known ^{1}H NMR spectrum of this compound published in other articles.[61] After this comparison it was realized that there were impurities present in the 9,10-bis(chloromethyl)anthracene sample

obtained from the German chemical company. If there were impurities present in the 9,10-BCA sample then this could explain why the bistren cage was not forming as a solid and was not pure. The impurities could be getting in the way of the cage formation or also aggregating to form the oil residue that was observed. However, since the product was not solid as described in the paper and the NMR did not seem correct, although there were no NMR data in the paper to compare it to, it was decided to look back through our procedure to check for possible sources of error.

During the first synthetic attempt there were a few steps that may have caused problems for the end result. Firstly, as mentioned above, the starting material was not pure. Secondly, the solution was inadvertently heated to reflux, so overheating might be a problem. This was the point where the initial brown residue was visible, which may have indicated that the product was slightly burnt. These two factors caused problems for further steps in the synthesis of the final product.

Although there were these synthetic issues and the 9,10-bis(chloromethyl)anthracene NMR indicated impurities, it was decided to try the synthesis again. This time there were precautions taken to attempt to prevent the same brown oily product from forming. In the second synthetic attempt the methanol solution was not allowed to boil, the temperature was increased slowly until it stabilized at 50°C. The solution remained yellow-orange this time without a brownish residue. This yellow-orange residue also dissolved much better in water, forming a milky yellow solution. The solution only needed to be sonicated for 20 minutes total and it was only dissolved in the 100 mL called for, no extra water was required for dissolving.

After rotary evaporation for an extra hour the resulting product this time was yellow-gold in color as desired but still oily. Therefore, the product was put under the higher vacuum rotary evaporator for a further 2 hours which resulted in a semi-solid yellow-gold product which was still a bit wet/oily but it was the best that could be obtained.

The solid formed was still sticky so it was dissolved in 40 mL 1M HCl and the solvent was evaporated again to see if we could obtain a solid product. After rotary evaporation for 3 hours a wet solid resulted so it was put on the higher vacuum rotary evaporator for 2 hours and the solid on the sides was yellow-gold and DRY. The solid was not crystalline but flaky.

V.2 *Characterization*

Now it was time to try and characterize the product. Since no NMR data were published, we could not simply rely on comparison of the spectra for identification. A sample of the product in D_2O was prepared for NMR and a ^1H NMR was run for 64 scans and a ^{13}C NMR was run overnight. Since there were no data for comparison a Chem Draw figure of the desired product was made and a simulation of the expected ^1H NMR spectrum was generated by the program. After comparing the ^1H NMR obtained on the sample and the Chem Draw simulation it was clear that the sample spectrum was not well defined and had impurities compared to the Chem Draw spectrum. The bistren cage may have been formed but it may not be pure and that is why the ^1H NMR was messy. The impurities may be due to the previously discovered impure 9,10-bis(chloromethyl)anthracene starting material. It may be that some was left unreacted or the impurities in the sample interfered

with cage production so the impurities are unformed intermediate cage products. Unfortunately a ^{13}C NMR could not be obtained on the product even after leaving it scanning overnight on a saturated sample so it was not available for comparison. At this stage there was little evidence that the bistren cage was indeed formed.

After performing these tests it was decided to consult colleagues to see what might be done to help purify and characterize the product. Following examination of the ^{1}H NMR results for the 9,10-bis(chloromethyl)anthracene starting material it was agreed that the 9,10-BCA compound ordered from ABCR in Germany was ~ 30% impure in the organic region. It was suggested that we contact the company for a more pure sample or for procedures for purification. The product made was believed to contain impurities and this impure starting material could be to blame. The impurities present in the starting compound could be either preventing cage formation in some cases so the cage product is contaminated with other unformed or half formed products.

Existing data and methods for purification and characterization were discussed further. It was already established that the ^{1}H NMR of the bistren product was not well defined and impurities were present so it was not very diagnostic. Also a ^{13}C NMR could not be obtained even though a saturated sample was left overnight and the rg was ~200. It was desired to perform 2D NMR for further characterization, however, it was realized that 2D-Carbon NMR cannot be performed unless a ^{13}C NMR can be obtained in only a few scans so this was not an option. In the article they gave Fast Atom Bombardment Mass Spectrometry data for characterization, unfortunately we do not have access to this in the chemistry department. Therefore colleagues at the NRC building were contacted about

running GC-MS, LC-MS and HPLC on the product to try and determine the composition of the product. As far as purification methods go it was determined that TLC could not be performed because the bistren host is basic so it is too polar to move through the plate. Also, elemental analysis cannot be performed on the product for identification because it is not pure.

In the mean time it was attempted to contact Fabbrizzi for characterization and fluorescence data but this attempt failed. The German company ABCR GmbH & KG Co was also contacted about purification methods for the 9,10-BCA they supplied, this was also unsucessful. So at this stage we were left with the possible HPLC results for characterization and the fluorescence results we obtained to verify our product is the desired bistren cage even if slightly impure.

The reason TLC could not be used for bistren characterization, as stated previously, was because the stationary phase is polar (normal phase) and the bistren cage is very polar so it would not travel up the plate at all therefore it could not be analysed. However, HPLC can be utilized if a reverse phase column is used because the stationary phase is non-polar and the mobile phase is polar. Therefore, the bistren cage would elute first from the column because it is very polar and would not stick to the column at all but dissolve and travel in the polar mobile phase.

HPLC data were collected by injecting a sample of bistren in a methanol:water gradient into the sample loop of the instrument. Trial one gave only one tiny peak, probably because the sample was too small. Therefore another 20μL sample was injected to increase the concentration. This trial yielded three peaks - one large peak and two small impurity

peaks. The large peak came off first as expected because it was the desired polar product. Peaks two and three were very small compared to the bistren peak indicating they are impurities. At this stage it was decided to perform three additional trials, this time collecting the peaks in vials as they eluted from the column and exit the absorbance detector. Then the vials would be placed in an evaporator to remove the solvent so the solid would remain for further NMR testing.

First a methanol blank was injected to see if any of the bistren peaks corresponded to solvent. The only peaks observed corresponded to the two impurities, probably from cross-contamination from the last bistren trial injection. Methanol was injected a second time and the impurity peaks were still present but weaker because the second methanol injection diluted the cross-contamination more.

This HPLC technique is very precise (reproducible) because the sample loop controls the amount of solvent added to the column. Three bistren samples were injected and the peaks collected and evaporated. This time a fourth peak was present showing another impurity. All four peaks can be seen in the chromatogram shown in Figure 25. After the peaks were dried the vials were re-weighed and the total weight of each peak from the different trials were added together to know how much of each peak was available for testing on the NMR. Peak 1 gave a total of 0.024 g, peak 2 - 0.0141 g, peak 3 - 0.0052 g and peak 4 - 0.0002 g.

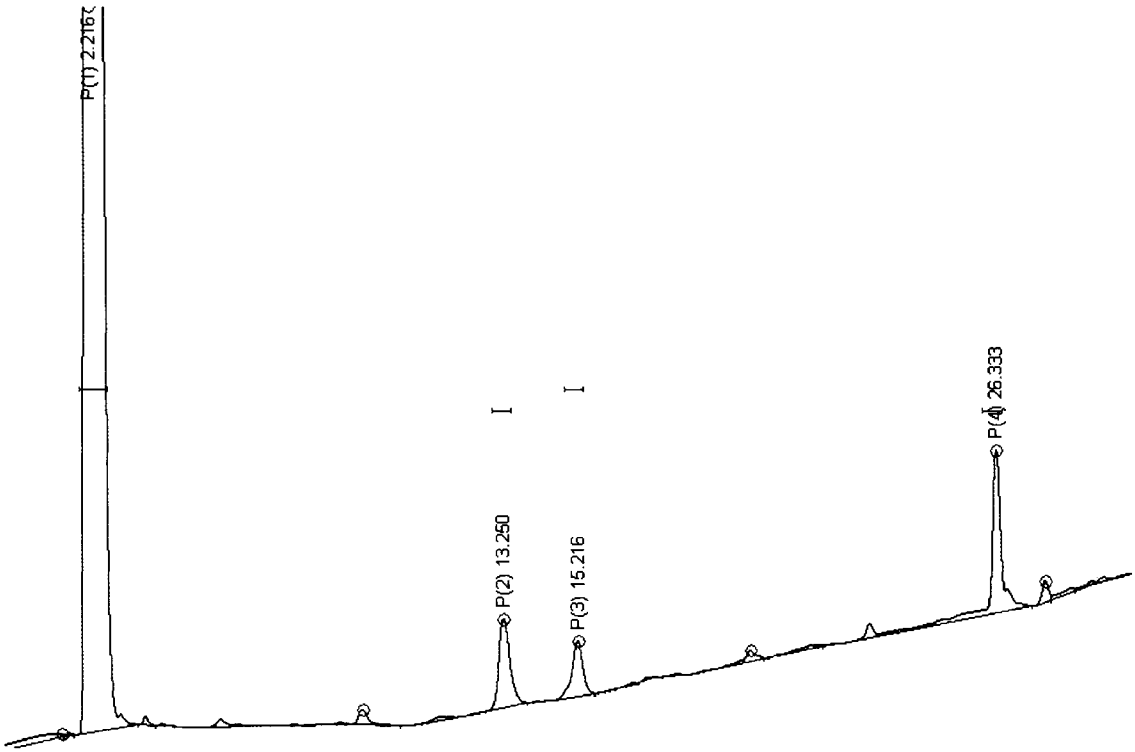

Figure 25 HPLC chromatogram of bistren cage

The Peak areas and % areas for this chromatogram are outlined in Table7 below:

Peak	**Total Area**	**% Area**
1	$6.74x10^4$	96.8
2	$7.14x10^2$	1.02
3	$4.26x10^2$	0.611
4	$1.12x10^3$	1.61

Table 7 Peak areas for bistren chromatogram

These area percentages show that the first peak is indeed the major product and that the remaining three peaks are very small impurities.

An NMR sample was made from the 24 mg peak 1 sample in 1 mL of D_2O to do both a ^{1}HNMR and a COSY to check for purity and structural characterization. This amount of sample should have been more than enough to get the NMR data. Although a ^{1}HNMR was obtained after 1024 scans (See Figure 27) a distinct COSY could not be obtained (See Figure 28). The peak 1 ^{1}HNMR when compared to the previous ^{1}HNMR, showed that the sample had fewer impurities so this should not present a problem when doing further fluorescence experiments. The following figure (Figure 26) and table (Table 8) help characterise the ^{1}HNMR seen in Figure 27.

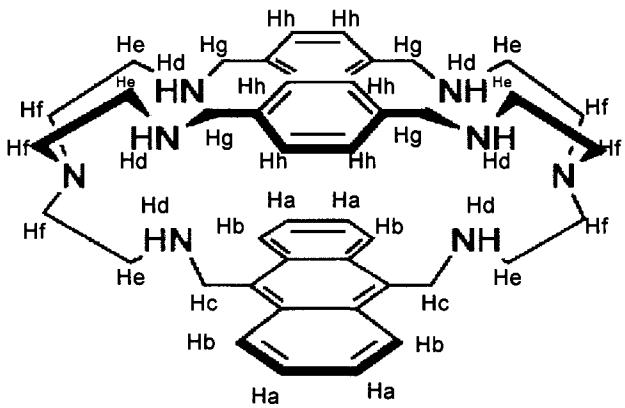

Figure 26 Bistren cage with protons labelled

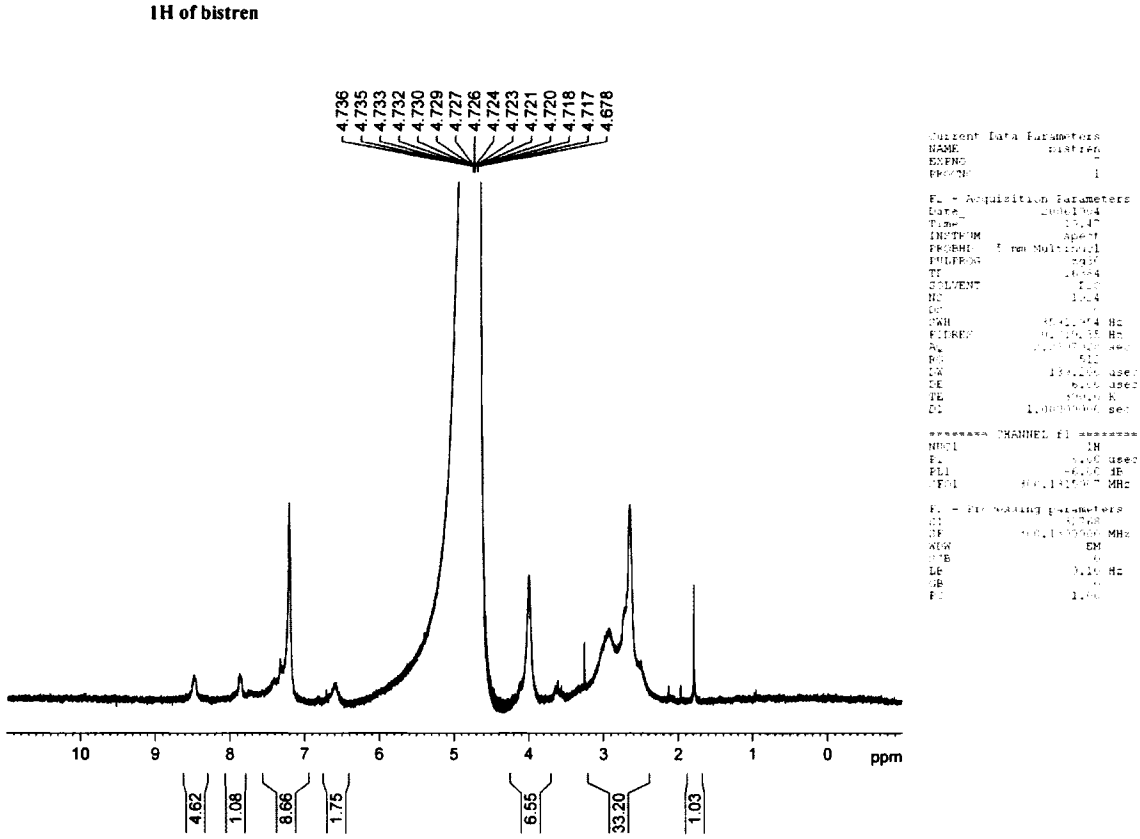

Figure 27 [1]HNMR spectrum of bistren cage

H	ppm
Hd	1.8
He, Hf	2.4-3.2
Hc, Hg	3.7-4.3
Ha, Hh	6.9-7.6
Hb	7.8-8.1

Table 8 Chemical shifts for [1]HNMR

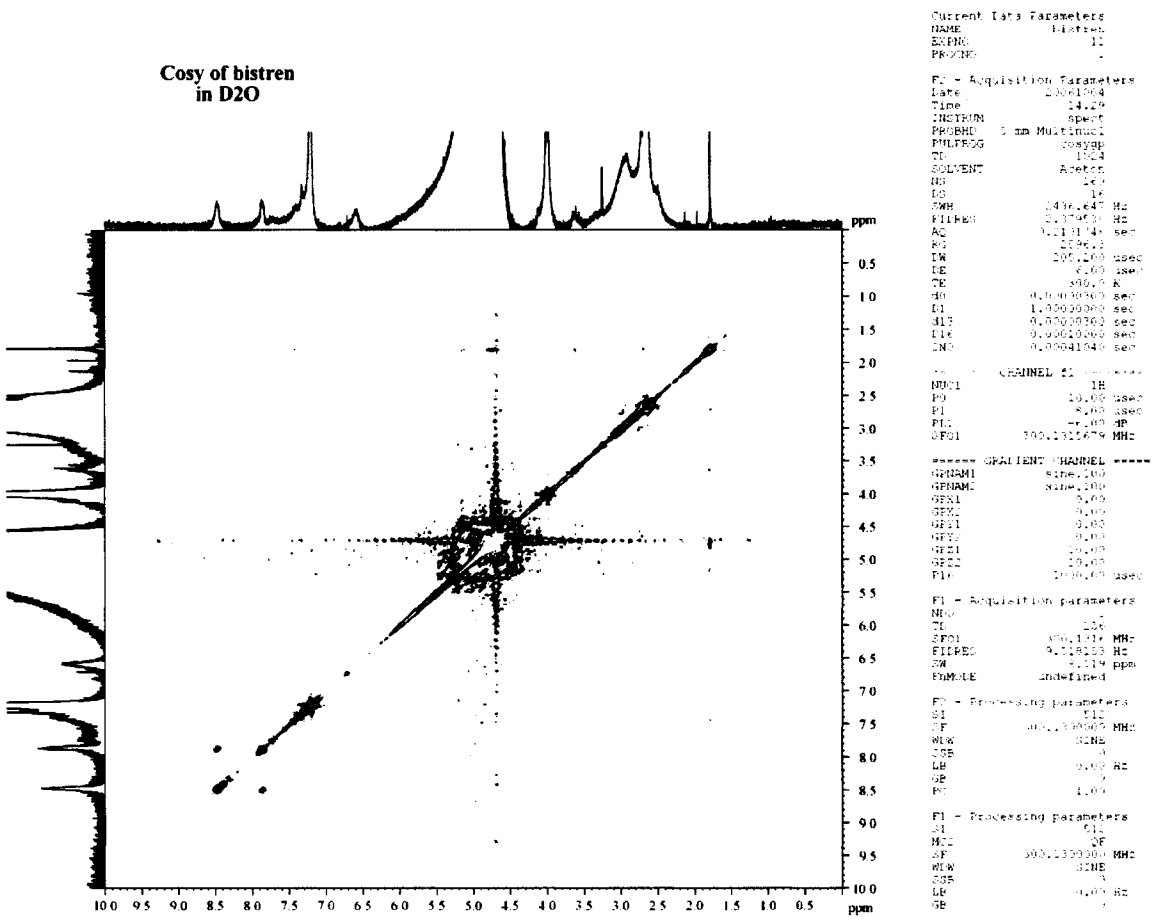

Figure 28 COSY spectrum of bistren cage

The following table (Table 9) outlines the proton correlations from the COSY seen in Figure 28.

H→H	H→H
Hd→Hd	Hh→Hh
He,Hf→He,Hf	Hb→Hb
Hc,Hg→Hc,Hg	

Table 9 Correlations for COSY

After examining the ^{1}HNMR it was a reasonable assumption that the desired bistren cage was indeed formed, even if the NMR was not very well defined. Also, interpretation of the COSY indicated that product was fairly symmetric which also leads to the assumption that the cage was formed.

At this point it was decided to go ahead with host-guest fluorescence experiments. According to the fluorescence experiments done in the paper the correct bistren cage was synthesized. Also the HPLC showed the cage was very pure and eluted in the correct location on the chromatogram. The bistren product also had the correct appearance as described in the synthetic procedure. It is proposed that Fabrizzi *et al.* also encountered problems with NMR characterization on the bistren and that is why they used FAB-MS instead. This may be why we encountered problems obtaining a ^{13}CNMR a COSY or a diagnostic ^{1}HNMR on this complex cage system.

V.3 *UV-Vis Absorption*

The absorption spectrum of the bistren cage was acquired and can be seen in Figure 29. Unlike the previous two hosts the bistren cage does not have a strong absorbance below 300 nm and absorbs between 340 nm and 410 nm. Therefore, a whole other range of guests become available to study. Bistren does not present the same problems as the other hosts in terms of guest absorbance overlapping with the host resulting in some guests not being available for study. For bistren, most common guests which absorb below 300 nm can indeed be studied.

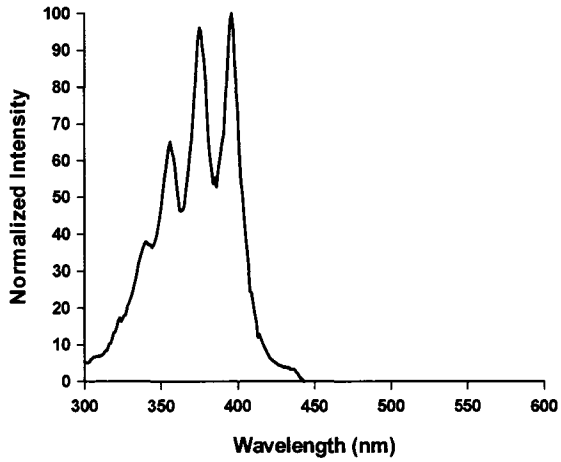

Figure 29 Absorption spectrum of bistren cage in water

V.4 *Steady-State Fluorescence*

The fluorescence spectrum of the bistren was obtained using λ_{ex}=340 nm and can be seen in Figure 30. This spectrum shows three fairly strong peaks at 400 nm, 423 nm and 447 nm. The peak at 423 nm is the most intense so therefore it was used for all further fluorescence studies.

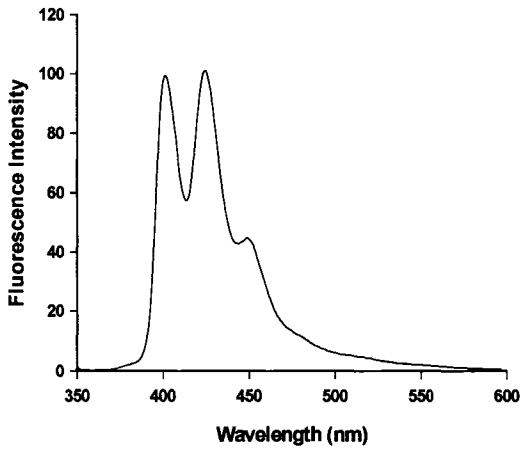

Figure 30 Fluorescence spectrum of bistren cage in water

In Trial 1 the absorbance and fluorescence spectra of the product were also obtained to see if it may be possible to determine whether the desired cage was made by comparing to the little fluorescence data outlined in the article. However, all this showed was that the product was fluorescent and since we had no λ_{Fmax} for comparison this did not tell us much. The starting material 9,10-bis(chloromethyl)anthracene and anthracene itself were tested for both absorbance and fluorescence for comparison to the product. This was done to see if there were any differences to indicate that the product was not simply starting material which would indicate a failed synthesis. The fluorescence spectrum of the product was different from that of both anthracene and the starting material. This confirms that there were changes made during the reaction so the product was different from the starting material which is a good sign.

For Trial 2 it was decided to try the solubility of the product in water, phosphate

buffer and acetate buffer which are the three solvents often used for our host-guest studies. The product was soluble in all three solvents but especially in water which is expected because of its acidic nature. Solubility was also tested in methanol for better comparison to the starting material which was not soluble in water. As before in Trial1 the product was fluorescent and when compared to the spectra of anthracene and 9,10-bis(chloromethyl)anthracene in methanol there was an obvious difference as seen in Figure 31. This is encouraging that the product is not the same as the starting material.

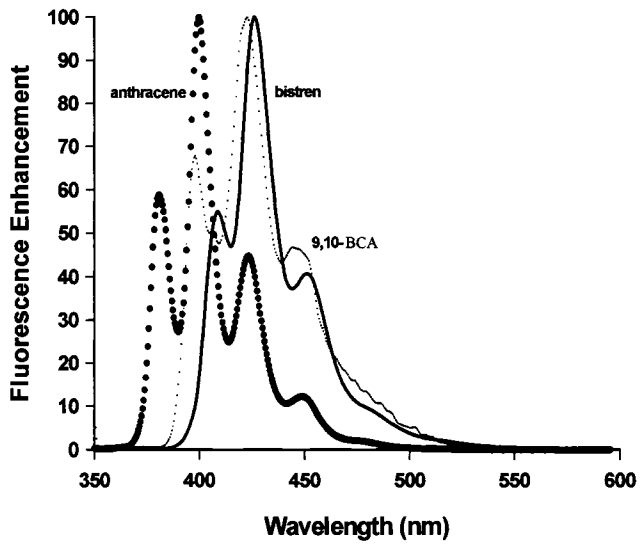

Figure 31 Bistren, 9,10-BCA and anthracene fluorescence in methanol

At this point it was decided to try and repeat the fluorescence experiments reported in the article. Although very few details were given the best attempt was made for reproduction. According to the paper 1 to 2 equivalents of sodium azide should quench the bistren fluorescence. Therefore approximately 2 equivalents of sodium azide was added to the solution and the fluorescence was retested to check the effect. This addition did in fact quench the fluorescence, the λ_{Fmax} band decreased in intensity from 101.37 to 4.41(See Figure 32). The sodium azide was also added to the anthracene and 9,10-bis(chloromethyl)anthracene solutions to see the effect. In this case the fluorescence actually increased which again show that the product does indeed differ from these compounds. Since neither anthracene or 9,10-BCA dissolved in water or gave a similar fluorescence signal to bistren and the fluorescence was not decreased by sodium azide it is safe to conclude that the bistren we made is different from the starting material and based on the sodium azide pattern it is probably the desired bistren cage.

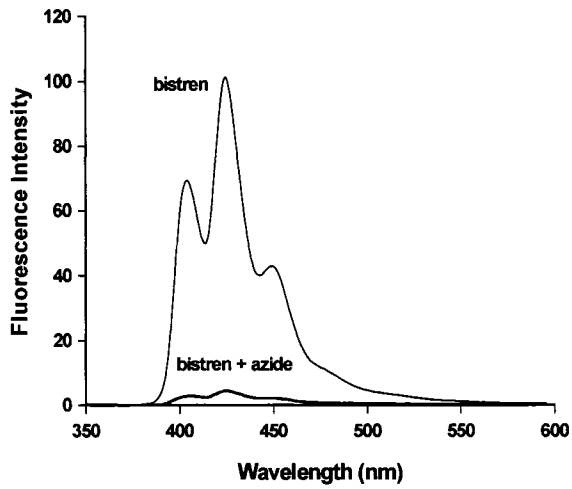

Figure 32 Fluorescence spectra of bistren and bistren+sodium azide in water

Also in the paper the fluorescence was tested in the presence of Zn(II) salts at varying pH solutions. The result was a large increase in fluorescence intensity of a pH 8.5 solution of the bistren cage in the presence of Zn(II). Therefore, a solution of bistren was made up at pH 8.5 and the fluorescence was tested. Then about 2 equivalents of zinc sulfate were added and the fluorescence did increase although not as much as reported in the article (See Figure 33). These tests indicate that based on the fluorescence properties the desired bistren cage has been made although NMR results were not well defined.

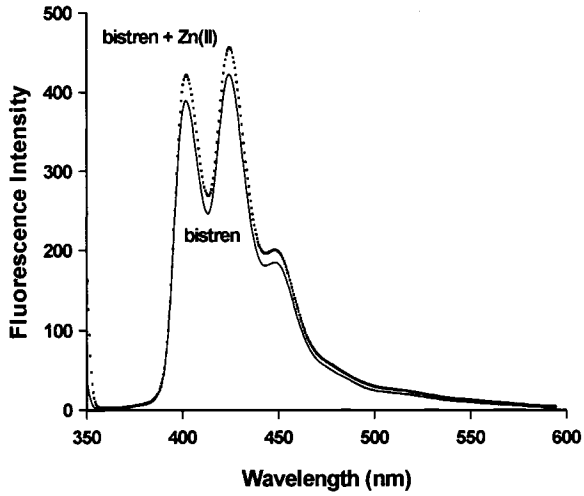

Figure 33 Fluorescence spectra of bistren and bistren+Zn(II) in pH 8.5 solution

V.5 *Host-Guest Fluorescence*

Unlike the previous two hosts discussed the bistren cage absorbs at higher wavelengths from 340-410 nm. Therefore guests which absorb below 300 nm can be examined with this host without overlap. The fluorescence of these guests was also checked in the same region as the host to ensure that there was no overlap before proceeding.

Initially as with the other two hosts, benzene was tried as a guest. The same set of concentrations 0-40 mM was used as with the other hosts, but resulted in only a very slight decrease in fluorescence intensity. Addition of benzene was of little significance to the bistren fluorescence and it was concluded that no complex was formed. At this time it was unclear why no complexation occurred between bistren and benzene. Therefore, it was decided to try other singly substituted benzene derivatives to see if they gave any effect on the bistren fluorescence.

The second guest attempted was phenol which is benzene with an OH substituent. Three trials were performed using concentrations from 0.0391-20 mM phenol in the host solution. Initially the concentrations ranged from 0.625-40 mM. However, the fluorescence dropped so dramatically upon the addition of just 0.625 mM phenol it was decided that an increased number of lower concentration solutions should be performed to try and fit the first part of the curve better. Unfortunately, this did not make much difference, the lower concentrations all remained around the same intensity as the 0.625 mM solution and were scattered, which did not help in the fitting process. Regardless, a 1:2 fit could be performed with large K_1 values and low chi squared values. The average fit parameters can be seen in Table 10.

Guest	σ_I	F_a	$K_1(M^{-1})$	F_b	K_2(M-1)	chisq
Aniline	0.12	0.30±0.13	$8.5x10^4$ $\pm 2.8x10^5$	0.00 ±0.06	8.1±31	0.01±0.02
Phenol	0.25	0.34±0.10	$4.6x10^5$ $\pm 1.0x10^8$	0.14 ±0.10	$1.3x10^2$ $\pm 1.2x10^2$	0.00 $\pm 1.6x10^{-3}$
Methyl Benzoate	0.31	0.94±0.00	$2.3x10^2$ ±0.00	0.92 ±0.00	11±0.00	0.00±0.00
Anisole	0.34	0.91±0.02	48±37	0.77 ±0.02	$1.5x10^2$ ±39	0.00 $\pm 1.2x10^{-4}$
Chlorobenzene	0.47	----------	----------	----------	---------	---------
Benzene	1	----------	----------	----------	---------	---------

Table 10 Inclusion constants and fit parameters for guests used

Aniline was the next guest attempted because it was thought that polarity may be the issue with guest binding and aniline polarity was thought to be between benzene and phenol. Again concentrations from 0.0391-40 mM were made in the bistren host solution. There were four trials performed because the first trial did not agree with the following three trials. As with the phenol there was a dramatic initial drop in fluorescence intensity. The lower concentrations, as with phenol, were scattered but a 1:2 fit was done and the results are shown in Table 10. The trend based on these three guests was thought to be based on polarity, and since benzene did not complex and phenol and aniline both complexed strongly, it was decided to try chlorobenzene, which was expected to give a similar result as benzene.

In the case of chlorobenzene, concentrations from 5-40 mM were made up in the

host solution. The resulting fluorescence titration resulted in no change in the fluorescence intensity and therefore no complexation. The trend based on these four guests was thought to be based on the substituent parameter σ_I, which is a measure of the inductive effect of the substituent on the benzene ring. The hypothesis was therefore made that the electron density of the substituted benzene π-system determines the strength of the binding. Therefore, the following guests were chosen according to their σ_I values between phenol (0.25) and chlorobenzene (0.47).

Anisole has a σ_I value of 0.34, so according to the predicted trend the K values should be between phenol and chlorobenzene giving a better, more gradual fit to the data. Concentrations of 5-40 mM anisole were made up in the bistren stock solution for three trials and the resulting fit, as predicted, was much better and more gradual as can be seen in Table 10 and Figure 34. It was desired to have another guest between phenol and anisole to complete the trend so methyl benzoate was chosen (σ_I=0.31).

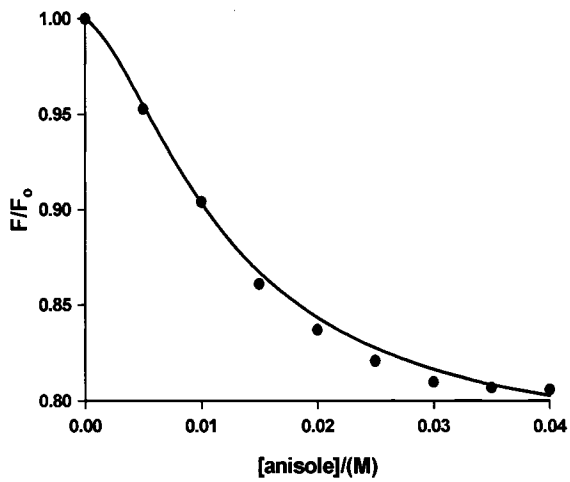

Figure 34 Average 1:2 fit for bistren+anisole

Four trials were performed with concentrations of methyl benzoate ranging from 5-40 mM. The first trial resulted in a very slow, small decrease in fluorescence intensity. However, the following three trials were scattered with some results going above the reference intensity and some below and others having no effect.

It was at this time that it was decided that there was more to the trend than just polarity or σ_I. A plot of both ln K_1 vs. σ_I and ln (K_1K_2) vs. σ_I were done but the data were scattered, not indicating a good trend. The plot of ln K_1 vs. σ_I is shown in Figure 35, the data follow the general trend but there is not a great correlation. A plot of ln K_1 vs. σ_R was also done, but again the data were scattered and were even less linear than with σ_I. Although there is obviously a substituent effect there must be more to the trend than inductive effect on the electronics of the dipole-dipole type interaction between the host and guest. Perhaps hydrogen bonding and other effects were involved which results in a much more complicated trend than can be predicted.

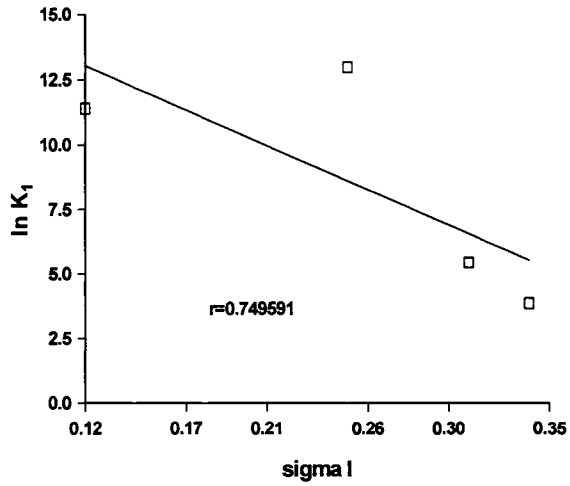

Figure 35 Bistren lnK_1 vs. σ_I

To ensure that these guest effects on the host were due to the entire host structure and not the starting material, both 9,10-bis(chloromethyl)anthracene and anthracene itself were titrated with aniline. This resulted in a small decrease in fluorescence intensity (F/F_o), but very little when compared with the bistren host (0.2 compared to 0.9). The decrease in host fluorescence upon guest inclusion depends on the entire cage structure because, as shown, the 9,10- fluorophore is unaffected by guest presence. There may be some electronic effect within the cage or excimer formation, but not direct quenching by the guest, the total effect is not known.

V.6 *Thermodynamics*

As discussed in the previous section, bistren forms a 1:2 complex with both anisole and phenol. Therefore, it was decided to examine these systems at 8, 15 and 32°C for comparison of K_1 values to those at 22°C. In the case of the anisole titrations , the K_1 value was increased to 233 M^{-1} at 8°C from the 48.4 M^{-1} obtained at 22°C. The K_1 value obtained at 15°C was 137 M^{-1} which agrees with the trend. At 32°C there was no fit done because no complex had formed, so essentially the K_1 value was even smaller than at room temperature which fits the trend. It was established that the K_1 value decreased with increasing temperature. The bistren-anisole system gave a good 1:2 fit so it was easier to establish a trend between the K_1 values and temperature.

For the bistren-phenol system, the binding is extremely strong so it was difficult to fit, but the K_1 value was 4.64×10^5 M^{-1} at 22°C. Unfortunately at 8°C the data could not be fit, possibly because the binding is so tight. Also, at 32°C the K_1 value actually increased

to 8.39×10^5 M^{-1}. In this case the binding constant K_1 is too large, therefore it cannot be measured reproducibly. Aniline, like phenol, also formed a strong complex with bistren. Therefore, it was not examined for thermodynamics due to the very strong binding. The other guests: methyl benzoate, chlorobenzene and benzene were not studied because they did not form a complex with bistren.

V.7 *Time-Resolved Fluorescence*

As discussed in the section V.5, bistren forms a 1:2 complex with aniline. The time-resolved fluorescence decays of both bistren and bistren with added 10, 20, 30 and 40 mM aniline were performed for comparison. Bistren itself had a fairly long lifetime of 5.66 ns. Upon addition of the 10 mM aniline the lifetime decreased to 1.17 ns, then down to 1.06 ns for 20 mM then 0.905 ns for 30 mM and finally 0.437 ns for 40 mM. The lifetimes of both bistren and bistren+40 mM aniline are shown in Figure 36. This result agrees with the steady-state fluorescence data which resulted in the F/F_o values decreasing dramatically from 1 to 0.150. Therefore, the non-radiative decay rate is increasing with the aniline concentration. This results in a decrease in quantum yield and fluorescence decay rate.

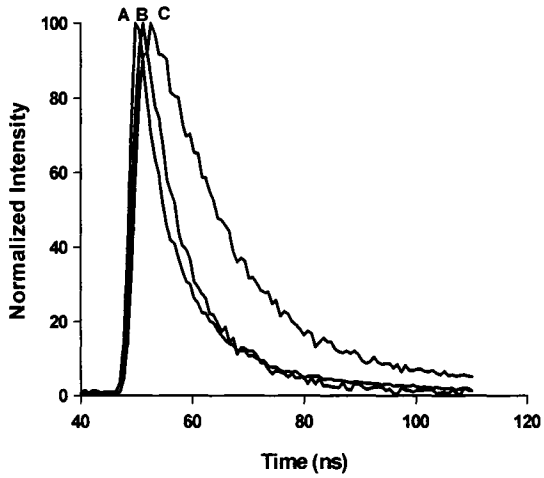

Figure 36 Time-resolved decay curves of **A** lamp profile, **B** bistren+40 mM aniline and **C** bistren

The lifetimes where aniline was present were all divided by the lifetime of bistren itself to give τ/τ_o values which were used to do a 1:2 fit on the time-resolved data; in much the same way that the F/F_o values were used to do a 1:2 fit on the steady-state data. The result was a good 1:2 fit with fluorescence suppression as seen in Figure 37. The resulting fit gave a K_1 value of $1.2x10^3 M^{-1}$ which is similar to that obtained through the steady state 1:2 fit, $K_1=8.5x10^4 M^{-1}$. The K_2 values in each case are also similar being 20 and 8.1 M^{-1} respectively. This is significant because this is the first time that the Wagner group has been able to use a time-resolved fluorescence titration to study the host-guest complex.

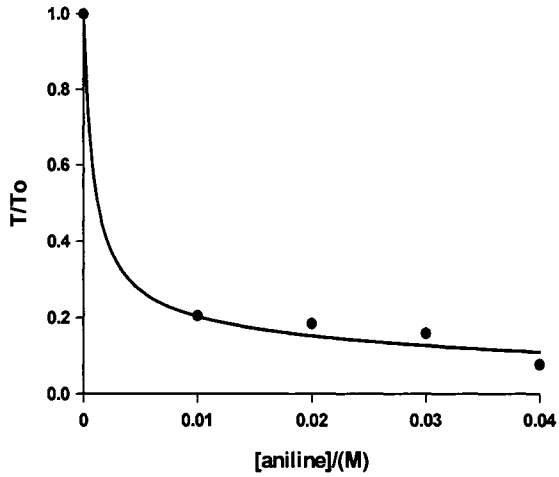

Figure 37 Time-resolved 1:2 fit for bistren+aniline

V.8 *Bistren Cage Conclusions*

Since this host was originally designed to detect the presence of anions there has be no work done with it outside this area. This allowed us to perform a whole series of unique experiments with this host and a wide range of different guests. Although only a few of the possible guests were studied during the course of this project there are numerous others which can be examined in future work. This fluorescent host unlike the other two hosts studied has no other articles published about its fluorescent properties with various guests so that leaves the field wide open for our future exploration.

Although there were some difficulties with the synthesis of the bistren cage it is believed that the correct product was made. The characterization was based on HPLC, ^{1}HNMR, COSY and fluorescence data. To the best of our knowledge and ability the desired bistren cage was synthesized, although further testing will be done on this host as new

techniques become available to us. The absorbance and fluorescence data in this case allow for a new range of guests to be studied which absorb below 300 nm. Time-resolved fluorescence data indicate a fairly long lifetime which is decreased by adding aniline, as expected.

As discussed, bistren forms 1:2 complexes with a variety of mono-substituted benzene derivatives. There was thought to be a trend in binding based on polarity and the substituent parameter, σ_I, but further experiments suggested that there was more to this trend, possibly hydrogen bonding and other effects which result in a much more complicated trend than can be predicted. Thermodynamics studies were also performed on a few of these host-guest systems. This indicated that the binding constant, K_1, was affected by the temperature, decreasing as temperature increased.

After the excellent results with the inclusion of a neutral molecule there is clearly further potential with this host both with neutral and possibly charged guests. This host has a charged nature due to the presence of the two tetramine units. Also during the final stages of synthesis the cage is dissolved in hydrochloric acid which leaves it highly charged in the hydrochloride salt form. The bistren cage was original designed to detect the presence of anions. Therefore, this host may be used to detect anionic guests such as 2,6-ANS. There is also potential for future work creating nanomachines using aniline based biphenyl molecules because of the tight binding seen with aniline.

VI. *Conclusion*

The three hosts which were investigated during this project each exhibited fluorescence properties. This is unusual because it is normally the guest which is fluorescent. Therefore this situation allows for the investigation of non-fluorescent guests, which is a whole new area of research for the Wagner group. The fluorescent guests can also be examined as before in areas of the spectrum where the host does not absorb or fluoresce. These fluorescent hosts have the potential to be used as fluorescent sensors for non-fluorescent guests and also to form nanomachines upon guest complexation.

The methoxy nanoball showed two peaks, one ligand centered and one assigned as an LMCT band. This latter band is of interest, as it is a result of the overall nanoball structure, and was found to have an intensity sensitive to the presence of guest molecules, making MNB a potential fluorescent sensor. Methoxy nanoball fluorescence also showed pH dependence where the second band only appeared above pH 5. This result could be promising for future work in the development of pH-dependent molecular switches, and is in itself a pH sensor. Since the MNB formed a weak 1:1 complex with only one small guest (benzene) it is unlikely that it would be of any further use in developing nanomachines or other fluorescence sensors. Maybe they could still have potential as fluorescent molecular switches or sensors, due to the pH dependence and sensitivity to the presence of guests. Also, the encapsulation of guests in the MNB structure during synthesis shows potential for future work and possible examination via x-ray crystallography.

The cucurbit[6]uril analogue examined also displayed fluorescence properties. This host formed a higher order complex with the fluorescent guest curcumin. It is possible that curcumin was joining the LB[6] host molecules together in a long chain, but crystal structures will have to be acquired for proof. The LB[6] is more likely to be used for the formation of nanomachines than the MNB because it formed higher order complexes with a larger aromatic guest. Thermodynamic and time-resolved results were also obtained. However, more work must be done in this area to reproduce the results if more LB[6] can be obtained by the research group.

The bistren cage synthesized during this project was also found to be fluorescent. Verification of the product identity was done through fluorescence data, HPLC and NMR. Bistren formed a 1:2 complex with phenol but did not form a complex with benzene. Therefore, this verifies that the desired bistren complex was formed because it did not complex all guests. It was specific for polar compounds because it was designed to detect anions. There was an unclear trend established between the guest substitution and the K_1 values due to various, as of yet undetermined, factors. Also a thermodynamic trend was established for anisole where the K value decreased with increasing temperature. Time-resolved data were also obtained with aniline which confirmed the steady-state results. Since this host forms higher order complexes as with LB[6] it may also be useful for the formation of nanomachines. This host shows potential for further neutral and possibly charged guest complexation.

The fluorescent properties of all three hosts were investigated. A series of aromatic guests were investigated with each host any complexes formed could potentially be used as

fluorescent sensors. Any higher order complexes formed have potential for the formation of nanomachines. Also any pH dependence could be used to develop pH sensors. All of these developments would be future work for the Wagner group.

VII. *References*

1. Lehn, J.M. *Agnew. Chem. Int. Ed. Engl.* **1988**, *27*, 89-112.

2. Moulton, B.; Lu, J.; Mondal, A.; Zaworotko, M.J. *Chem. Commun,* **2001**, 863-864.

3. McManus, G.J.; Zhenquiang, W.; Zaworotko, M.J. *Cryst.Growth Des.* **2003**, 1-3.

4. Smithrud, D.B.; Diederich, F. *J. Am. Chem. Soc.* **1990**, *112*, 339-343.

5. Forman, J.E.; Marsh, R.E.; Schaefer, W.P.; Dougherty, D.A. *Acta Crytallogr* **1993**, *B49*, 892-896.

6. Abe, H.; Mawatari, Y.; Teraoka, H.; Fujimoto, K.; Inouye, M. *J. Org. Chem.* **2004**, *69*, 495-504.

7. Fabbrizzi, L.; Faravelli, I.; Francese, G.; Licchelli, M.; Perotti, A.; Taglietti, A. *Chem. Commun.* **1998**, 971-972.

8. Lehn, J.M. Supramolecular Chemistry: Concepts and Perspectives, VCH: New York 1995.

9. Tabushi, I.; Kiyosuke, Y.; Sugimoto, T.; Yamamura, K. *J. Am. Chem. Soc.* **1978**, *100*, 916-919.

10. Berr, P.D.; Gale, P.A.; Smith, D.K. Supramolecular Chemistry, London: Oxford Science Publications 1999.

11. De La Pena, A.M.; Salinas, F.; Gomez, M.J.; Aceda, M.I.; Pena, M.S. *J. Inclus. Phenom.Mol.Rec.Chem.* **1993**, *15*, 131-143.

12. Wagner, B.D. Fluorescence Studies of Supramolecular Host-Guest Inclusion Complexes in *Handbook of Photochemistry and Photobiology*; Nalwa, H.S., Ed.; American Scientific Publishers: New York, 2003; pp 1-57.

13. Spanggard, H. *Introduction to Fluorescence*, http://www.risoe.dk/pol/competence/chemanal/fls920.pdf Accessed 15/01/2005

14. O'Connor, D.V.; Phillips, D. *Time-correlated Single Photon Counting*; Academic Press: London, 1984; pp 1-35

15. *Spectroscopy*; Straughan, B.P.; Walker, S., Ed.; Chapman and Hall: Newcastle, 1976; pp 161-198.

16. Englman, R.; Jortner, J. *Mol. Phys.* **1970**, *18*, 145.

17. Wagner, B.D.; MacDonald, P.J. *J. Photochem. Photobiol. A* **1998**, 114, 151-157.

18. Benesi, H.A.; Hildebrand, H. *J. Am. Chem. Soc.* **1949**, *71*, 2703-2707.

19. Nigam, S.; Durocher, G. *J. Phys. Chem.* **1996**, *100*, 7135-7142.

20. Boland, P.G. "Fluorescence Investigations of Various Substituted Nanoballs", Honours Thesis, UPEI, April 2005.

21. Freeman, W.A.; Mock, W.L.; Shih, N.Y. *J. Am. Chem. Soc.* **1981**, *103*, 7367-7368.

22. Mock, W.L. *Top. Curr. Chem.* **1995**, *175*, 1-24.

23. Mock, W.L.; Shih, N.-Y. *J. Org. Chem.* **1983**, *48*, 3618-3619.

24. Mock, W.L.; Shih, N.-Y. *J. Am. Chem. Soc.* **1988**, *110*, 4706-4710.

25. Mock, W.L.; Shih, N.-Y. *J. Am. Chem. Soc.* **1989**, *111*, 2697-2699.

26. Buschmann, H.-J.; Jansen, K.; Meschke, C.; Schollmeyer, E. *J. Solution Chem.* **1998**, *27*, 135-140.

27. Buschmann, H.-J.; Schollmeyer, E. *J. Inclusion Phenom. Mol. Recognit. Chem.* **1997**, *29*, 167-174.

28. Whang, D.; Jeon, Y.-M.; Heo, J.; Kim, K. *J. Am. Chem. Soc.* **1996**, *118*, 11333-11334.

29. Whang, D.; Kim, K. *J. Am. Chem. Soc.* **1997**, *119*, 451-452.

30. Whang, D.; Heo, J.; Kim, C.-A.; Kim, K. *Chem. Commun.* **1997**, 2361-2362.

31. Mock, W.L.; Shih, N.-Y. *J. Org. Chem.* **1986**, *51*, 4440-4446.

32. Hoffmann, R.; Knoche, W.; Fenn, C.; Buschmann, H.-J. *J. Chem. Soc., Faraday Trans.* **1994**, *90*, 1507-1511.

33. Meschke, C.; Buschmann, H.-J.; Schollmeyer, E. *Thermochim. Acta* **1997**, *297*, 43-48.

34. Buschmann, H.-J.; cleve, E.; Schollmeyer, E. *Inorg.Chim. Acta* **1992**, *193*, 93-97.

35. Buschmann, H.-J.; Jansen, K.; Schollmeyer, E. *Thermochim. Acta* **1998**, *317*, 95-98.

36. Neugebauer, R.; Knoche, W. *J. Chem. Soc., Perkins Trans. 2* **1998**, 529-534.

37. Wagner, B.D.; MacRae, A.I. *J. Phys. Chem. B* **1999**, *103*, 10114-10119.

38. Wagner, B.D.; Fitzpatrick, S.J.; Gill, M.A.; MacRae, A.I.; Stojanovic, N. *Can. J. Chem.* **2001**, *79*, 1101-1104.

39. Wagner, B.D.; Stojanovic, N.; Day, A.I.; Blanch, R.J. *J. Phys.Chem. B* **2003**, *107*, 10741-10746.

40. Rankin, M.A.; Wagner, B.D. *Supramol. Chem.* **2004**, *16*, 513-519.

41. Jun, S.I.; Lee, J.W.; Sakamoto, S.; yamaguchi, K.; Kim, K. *Tetrahedron Lett.* **2000**, *41*, 471-475.

42. Jon, S.Y.; Selvapalam, N.; Oh, D.H.; Kang, J.-K.; Kim, S.-Y.; Jeon, Y.J.; Lee, J.W.; Kim, K. *J. Am. Chem. Soc.* **2003**, *125*, 10186-10187.

43. Buschmann, H.-J.; Wolff, T.J. *Photochem. Photobiol., A* **1999**, *121*, 99-103.

44. Marquez, C.; Huang, F.; Nau, W.M. *IEEE Trans. Nanobiosci.* **2004**, *3*, 39-45.

45. Lagona, J.; Fettinger, J.C.; Isaacs, L. *Organic Letters* **2003**, *5* (20), 3745-3747.

46. Wagner, B.D.; Boland, P.G.; Lagona, J.; Isaacs, L. *J. Phys. Chem. B* **2005**, *109*, 7686-7691.

47. De Santo, G.; Fabbrizzi, L.; Perotti, A.; Sardono, N.; Taglietti, A. *Inorg. Chem.* **1997**, *36*, 1998-2003.

48. Burnett, C.A.; Lagona, J.; Wu, A.; Shaw, J.A.; Coady, D.; Fettinger, J.C.; Day, A.J.; Isaacs, L. *Tetrahedron* **2003**, *59*(11), 1961-1970.

49. Drew, H.D.K.; Pearman, F.H. *J. Chem. Soc.* **1937**, 586-592.

50. Fabrizzi, L.; Francese, G.; Licchelli, M.; Perotti, A.; Taglietti, A. *Chem. Commun.* **1997**, 581-582.

51. Miessler, G.L.; Tarr, D.A. *Inorg. Chem.*;Pearson Prentice Hall: New Jersey, **2004**;pp 407-408.

52. Kunkely, H.; Volger, A. *Inorganica Chimica Acta* **2004,** *357*, 888-890.

53. Cheruzel, L.E.; Cecil, M.R.; Edison, S.E.; Mashuta, M.S.; Baldwin, M.J.; Buchanan, R.M. *Inorg. Chem.* **2006**, *45*, 3191-3202.

54. Zhu, S.S.; Carroll, P.J.; Swager, T.M. *J. Am. Chem. Soc.* **1996**, *118*, 8713-8714.

55. Kalyanasundaram, K.; Thomas, J.K. *J. Am. Chem. Soc.* **1977**, *99*, 2039-2044.

56. Lagona, J.; Wagner, B.D.; Isaacs, L. *J. Org. Chem.* **2006**, *71*, 1181-1190.

57. Baglole, K.N.; Boland, P.G.; Wagner, B.D. *J. Photochem. Photobiol. A: Chemistry* **2005**, *173*, 230-237.

58. Rankin, M.A.; Wagner, B.D. *Supramol.Chem.* **2004**, *16*, 513-519.

59. Loukas, Y.L. *J. Phys. Chem. B* **1997**, *101*, 4863-4866.

60. Hamai, S.; Hatamiya, A. *Bull. Chem. Soc. Jpn.* **1996**, *69*, 2469-2476.

61. Kim, C.S.; Oh, S.M.; Kim, S.; Cho, C.G. *Macromol. Rapid Commun.* **1998**, *19*, 191-196.